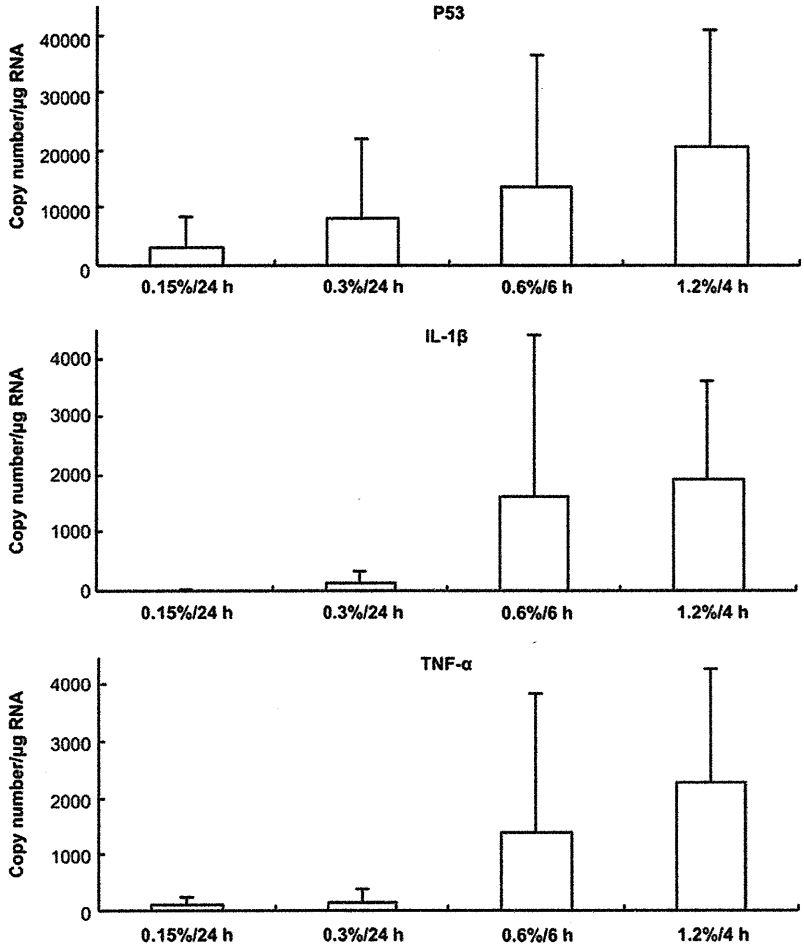

FIG. 5. Gene expression of the proapoptotic factor and the inflammatory cytokines. Gene expression of the proapoptotic factor, p53, or the inflammatory cytokines, tumor necrosis factor alpha (TNF-α), and interleukin 1beta (IL-1β) tended to be upregulated in the chondrocytes as the concentration of collagenase increased. All values are presented as mean ± SD of three samples per group.

gest. The mincing damaged the cells located on the surface of the tissues and decreased the viability of those cells. Therefore, the cells harvested after the 2 h incubation period showed a low viability (Fig. 2C). This tendency was also confirmed by the results of apoptosis assay. When the chondrocytes were exposed to lower concentrations of collagenase (0.15% or 0.3%), in which the cytotoxic effects of collagenase may hardly become obvious, those of short-term exposure (2–4 h) showed rather high extent of apoptosis (Fig. 6).

The cytotoxic effects of long-term exposure to collagenase were regarded as the cause of decrease in the viable cell numbers for those cells harvested at 24 h in 1.2% collagenase. In the present study, the maximum number of cells harvested from the native cartilage was $\sim 1 \times 10^7$ cells/g. These cell numbers were lower than those found in human cartilage (1×10^8 cells/g[31]), but it is a 10-fold increase when compared to previous data (1×10^6 cells/g[26]).

A cell density of 30,000 cells/cm^2 upon seeding was regarded as too high because the cells harvested from the

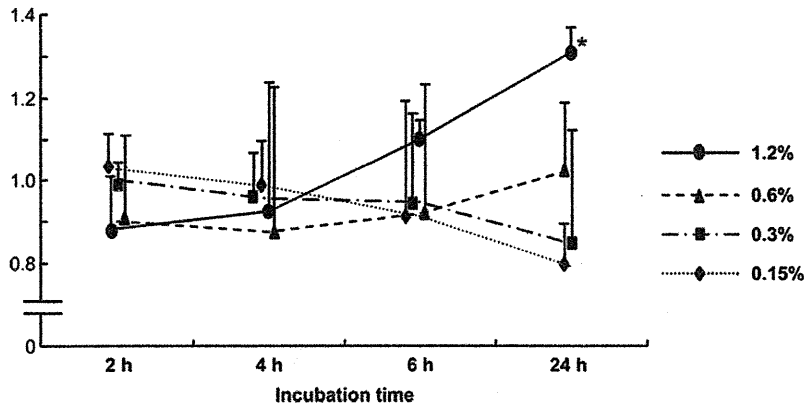

FIG. 6. Apoptosis enzyme-linked immunosorbent assay. Apoptosis appeared to be increased after digestion in 1.2% collagenase, especially at 24 h. All values are presented as mean ± SD of three samples per group. Statistics were assessed using the Dunnett's test (*$p < 0.05$, vs. 2 h in each concentration of collagenase).

0.6% to 1.2% collagenase digest tended to be aggregated, as seen in Figure 3. If fragments of the matrices remain around the chondrocytes after collagenase digestion, the chondrocytes may aggregate because cell aggregation is promoted by the matrix fragments that mediate the cell–matrix interaction.[38] Exposure to a higher concentration of collagenase even for a short incubation period could completely release the chondrocytes, but some fragments of the extracellular matrices may remain, which could mediate cell aggregation in a cell density as high as 30,000 cells/cm^2. In contrast, the density of 3000–10,000 cells/cm^2 showed appropriate adhesion and subsequent proliferation in all concentrations.

In addition, for a cell density lower than 1000 cells/cm^2, some viable cells were obtained after more than a week of incubation, as shown in Figure 4B.

It took 2 weeks for cells at initial densities <1000 cells/cm^2 to become confluent, and cells seeded at 100 cells/cm^2 needed as long as 3 weeks (Fig. 4B). However, if it takes >2 weeks for the chondrocytes to become confluent after seeding, too much time may be spent judging whether or not the chondrocytes have appropriately proliferated. A cell density at which the cells completely reach confluence within 1 week is desirable. Moreover, the paracrine/autocrine signals are needed for adequate cell proliferation.[39] Cells may not sufficiently proliferate at a low cell density because they cannot receive the paracrine/autocrine signals from adjacent cells. On the other hand, when the cell density is higher than 10,000 cells/cm^2, the passage would be needed at <1 week of incubation. If the incubation time during one passage is shortened and the passage number increases correspondingly, procedures become more complicated, and the risk of dedifferentiation may increase.

p53 and Bcl-2 are related to apoptosis. p53 induces apoptosis, participating in the maintenance of cell homeostasis.[33] Bcl-2, on the other hand, prohibits apoptosis.[34] TNF-α and IL-1β are inflammatory cytokines that are synthesized by natural immune cells in response to the infection or destruction of tissues.[35,36] Analysis of gene expression of these inflammatory cytokines, apoptosis-related molecules and apoptosis assay revealed that damage to the cells is diminished when the collagenase concentration is low. The damage to the cells may result from the cytotoxicity of the collagenase, which is a kind of digestive enzyme.

Therefore, we recommend a 24-h incubation in 0.3% collagenase, or 6 h in 0.6% collagenase, as the optimal condition for chondrocyte isolation from cartilage pieces that are 250–1000 μm in size. Moreover, the cell-seeding density should be in the range of 3000–10,000 cells/cm^2. These conditions maximize the harvest of the isolated chondrocytes from a small amount of biopsied tissue and significantly aid in obtaining a large quantity of cultured cells in a short period.

Acknowledgments

We thank Mr. Takashi Nakamoto, Ms. Miki Akizawa, Mr. Tomoaki Sakamoto, Mr. Takayuki Furuichi, and Mr. Makoto Watanabe for their technical support. This work was supported by Grants-in-Aid for Scientific Research from the Ministry of Education, Culture, Sports, Science and Technology of Japan (MEXT, No. 21390532 and 21659462), Research and Development Programs for Three-dimensional Complex Organ Structures from the New Energy and Industrial Technology Development Organization, and Resolving Critical Issues from Special Coordination Funds for Promoting Science and Technology (SCF) commissioned by MEXT.

Disclosure Statement

No competing financial interests exist.

References

1. Huckle, J., Dootson, G., Medcalf, N., McTaggart, S., Wright, E., Carter, A., Schreiber, R., Kirby, B., Dunkelman, N., Stevenson, S., Reiley, S., Davisson, T., and Ratcliffe, A. Differentiated chondrocytes for cartilage tissue engineering. Novartis Found Symp **249,** 103, 2003.
2. Asawa, Y., Ogasawara, T., Takahashi, T., Yamaoka, H., Nishizawa, S., Matsudaira, K., Mori, Y., Takato, T., and Hoshi, K. Aptitude of auricular and nasoseptal chondrocytes cultured under a monolayer or three-dimensional condition for cartilage tissue engineering. Tissue Eng Part A **15,** 1109, 2009.
3. Ruszymah, B.H.I., Lokman, B.S., Asma, A., Munirah, S., Chua, K., Mazlyzam, A.L., Isa, M.R., Fuzina, N.H., and Aminuddin, B.S. Pediatric auricular chondrocytes gene expression analysis in monolayer culture and engineered elastic cartilage. Int J Pediatr Otorhinolaryngol **71,** 1225, 2007.
4. Ruszymah, B.H.I., Chua, K.H., Mazlyzam, A.L., Fuzina, N.H., and Aminuddin, B.S. Formation of *in vivo* tissue-engineered human hyaline cartilage in the shape of a trachea with internal support. Int J Pediatr Otorhinolaryngol **69,** 1489, 2005.
5. Park, S.S., Jin, H.R., Chi, D.H., and Taylor, R.S. Characteristics of tissue-engineered cartilage from human auricular chondrocytes. Biomaterials **25,** 2363, 2004.
6. Yanaga, H., Yanaga, K., Imai, K., Koga, M., Soejima, C., and Ohmori, K. Clinical application of cultured autologous human auricular chondrocytes with autologous serum for craniofacial or nasal augmentation and repair. Plast Reconstr Surg **117,** 2019, 2006.
7. Rodriguez, A., Cao, Y.L., Ibarra, C., Pap, S., Vacanti, M., Eavey, R.D., and Vacanti, C.A. Characteristics of cartilage engineered from human pediatric auricular cartilage. Plast Reconstr Surg **103,** 1111, 1999.
8. Kamil, S.H., Woda, M., Bonassar, L.J., Novitsky, Y.W., Vacanti, C.A., Eavey, R.D., and Vacanti, M.P. Normal features of tissue-engineered auricular cartilage by flow cytometry and histology: patient safety. Otolaryngol Head Neck Surg **129,** 390, 2003.
9. Kamil, S.H., Rodrigruez, A., Vacanti, C.A., Eavey, R.D., and Vacanti, M.P. Expansion of the number of human auricular chondrocytes: recycling of culture media containing floating cells. Tissue Eng **10,** 139, 2004.
10. Kamil, S., Kojima, K., Vacanti, M., Zaporojan, V., Vacanti, C., and Eavey, R. Tissue-engineered cartilage: utilization of autologous serum and serum-free media for chondrocyte culture. Int J Pediatr Otorhinolaryngol **71,** 71, 2007.
11. Kamil, S.H., Vacanti, M.P., Vacanti, C.A., and Eavey, R.D. Microtia chondrocytes as a donor source for tissue-engineered cartilage. Laryngoscope **114,** 2187, 2004.
12. Cao, Y.L., Vacanti, J.P., Paige, K.T., *et al.* Transplantation of chondrocytes utilizing a polymer-cell construct to produce tissue-engineered cartilage in the shape of a human ear. Plast Reconstr Surg **100,** 297, 1997.

13. Ochi, M., Uchio, Y., Kawasaki, K., Wakitani, S., and Iwasa, J. Transplantation of cartilage-like tissue made by tissue engineering in the treatment of cartilage defects of the knee. J Bone Joint Surg Br **84,** 571, 2002.
14. Shieh, S.J., Terada, S., and Vacanti, J.P. Tissue engineering auricular reconstruction: *in vitro* and *in vivo* studies. Biomaterials **25,** 1545, 2002.
15. Rotter, N., Bonassar, L.J., Tobias, G., Lebl, M., Roy, A.K., and Vacanti, C.A. Age dependence of cellular properties of human septal cartilage: implications for tissue engineering. Arch Otolaryngol Head Neck Surg **127,** 1248, 2001.
16. Yoo, S.A., Park, B.H., Yoon, H.J., Lee, J.Y., Song, J.H., Kim, H.A., Cho, C.S., and Kim, W.U. Calcineurin modulates the catabolic and anabolic activity of chondrocytes and participates in the progression of experimental osteoarthritis. Arthritis Rheum **56,** 2299, 2007.
17. Liu, G., Kawaguchi, H., Ogasawara, T., Asawa, Y., Kishimoto, J., Takahashi, T., Chung, U.I., Yamaoka, H., Asato, H., Nakamura, K., Takato, T., and Hoshi, K. Optimal combination of soluble factors for tissue engineering of permanent cartilage from cultured human chondrocytes. J Biol Chem **282,** 20407, 2007.
18. Takahashi, T., Ogasawara, T., Asawa, Y., Mori, Y., Uchinuma, E., Takato, T., and Hoshi, K. Three-dimensional microenvironments retain chondrocyte phenotypes during proliferation culture. Tissue Eng **13,** 1583, 2007.
19. Yamaoka, H., Asato, H., Ogasawara, T., Nishizawa, S., Takahashi, T., Nakatsuka, T., Koshima, I., Nakamura, K., Kawaguchi, H., Chung, U.I., Takato, T., and Hoshi, K. Cartilage tissue engineering using human auricular chondrocytes embedded in different hydrogel materials. J Biomed Mater Res A **78, 1,** 2006.
20. Van Osch, G.J., Van der Veen, S.W., and Verwoerd-Verhoef, H.L. *In vitro* redifferentiation of culture-expanded rabbit and human auricular chondrocytes for cartilage reconstruction. Plast Reconstr Surg **107,** 433, 2001.
21. Moskalewski, S., and Thyberg, J. Reversible changes in nuclear and cell surface topography in cells exposed to collagenase and EDTA. Cell Tissue Res **220,** 51, 1981.
22. Brittberg, M., Nilsson, A., Lindahl, A., Ohlsson, C., and Peterson, L. Rabbit articular cartilage defects treated with autologous cultured chondrocytes. Clin Orthop **326,** 270, 1996.
23. Naumann, A., Dennis, J.E., Aigner, J., Coticchia, J., Arnold, J., Berghaus, A., Kastenbauer, E.R., and Caplan, A.I. Tissue engineering of autologous cartilage grafts in three-dimensional *in vitro* macroaggregate culture system. Tissue Eng **10,** 1695, 2004.
24. Johnson, T.S., Xu, J.W., Zaporojan, V.V., Mesa, J.M., Weinand, C., Randolph, M.A., Bonassar, L.J., Winograd, J.M., and Yaremchuk, M.J. Integrative repair of cartilage with articular and nonarticular chondrocytes. Tissue Eng **10,** 1308, 2004.
25. Brittberg, M., Lindahl, A., Nilsson, A., Ohlsson, C., Isaksson, O., and Peterson, L. Treatment of deep cartilage defects in the knee with autologous chondrocyte transplantation. N Engl J Med **331,** 889, 1994.
26. Peterson, L., Minas, T., Brittberg, M., *et al.* Two- to 9-year outcome after autologous chondrocyte transplantation of the knee. Clin Orthop **374,** 212, 2000.
27. Hayes, A.J., Hall, A., Brown, L., Tubo, R., and Caterson, B. Macromolecular organization and *in vitro* growth characteristics of scaffold-free neocartilage grafts. J Histochem Cytochem **55,** 853, 2007.
28. Melero-Martin, J.M., Dowling, M.-A., Smith, M., and Al-Rubeai, M. Expansion of chondroprogenitor cells on macroporous microcarriers as an alternative to conventional monolayer systems. Biomaterials **27,** 2970, 2006.
29. Chia, S., Homicz, M., Schumacher, B., Thonar, E., Masuda, K., Sah, R., *et al.* Characterization of human nasal septal chondrocytes cultured in alginate. J Am Coll Surg **200,** 691, 2005.
30. Alexander, T., Sage, A., Schumacher, B., Sah, R., and Watson, D. Human serum for tissue engineering of human nasal septal cartilage. Otolaryngol Head Neck Surg **135,** 397, 2006.
31. Bassermann, F., Frescas, D., Guardavaccaro, D., Busino, L., Peschiaroli, A., and Pagano, M. The Cdc14B-Cdh1-Plk1 axis controls the G2 DNA-damage-response checkpoint. Cell **134,** 256, 2008.
32. Tanaka, Y., Ogasawara, T., Asawa, Y., Yamaoka, H., Nishizawa, S., Mori, Y., Takato, T., and Hoshi, K. Growth factor contents of autologous human sera prepared by different production methods and their biological effects on chondrocytes. Cell Biol Int **32,** 505, 2008.
33. Oda, K., Arakawa, H., Tanaka, T., Matsuda, K., Tanikawa, C., Mori, T., Nishimori, H., Tamai, K., Tokino, T., Nakamura, Y., and Taya, Y. p53AIP1, a potential mediator of p53-dependent apoptosis, and its regulation by Ser-46-phosphorylated p53. Cell **102,** 849, 2000.
34. Kinnally, K.W., and Antonsson, B. A tale of two mitochondrial channels, MAC and PTP, in apoptosis. Apoptosis **12,** 857, 2007.
35. Locksley, R.M., Killeen, N., and Lenardo, M.J. The TNF and TNF receptor superfamilies: integrating mammalian biology. Cell **104,** 487, 2001.
36. Morgan, M.M., Clayton, C.C., and Heinricher, M.M. Dissociation of hyperalgesia from fever following intracerebroventricular administration of interleukin-1beta in the rat. Brain Res **1022,** 96, 2004.
37. Ross, M.H., Romrell, L.J., and Kaye, G.I. Histology: A Text and Atlas, 3rd edition. Baltimore, MD: Williams & Wilkins, 1995.
38. Steck, E., Br Bun, J., Pelttari, K., Kadel, S., Kalbacher, H., and Richter, W. Chondrocyte secreted CRTAC1: a glycosylated extracellular matrix molecule of human articular cartilage. Matrix Biol **26,** 30, 2007.
39. Olney, R.C., Wang, J., Sylvester, J.E., and Mougey, E.B. Growth factor regulation of human growth plate chondrocyte proliferation *in vitro*. Biochem Biophys Res Commun **317,** 1171, 2004.

Address correspondence to:
Kazuto Hoshi, M.D., Ph.D.
Department of Cartilage and Bone Regeneration (Fujisoft)
Graduate School of Medicine
University of Tokyo
Hongo 7-3-1, Bunkyo-ku
Tokyo 113-8655
Japan

E-mail: pochi-tky@umin.net

Received: September 4, 2009
Accepted: April 20, 2010
Online Publication Date: October 28, 2010

Biomaterials 31 (2010) 8004–8011

Contents lists available at ScienceDirect

Biomaterials

journal homepage: www.elsevier.com/locate/biomaterials

The influence of skeletal maturity on allogenic synovial mesenchymal stem cell-based repair of cartilage in a large animal model

Kazunori Shimomura [a], Wataru Ando [a], Kosuke Tateishi [a], Ryosuke Nansai [b], Hiromichi Fujie [b], David A. Hart [c], Hideyuki Kohda [a], Keisuke Kita [a], Takashi Kanamoto [a], Tatsuo Mae [a], Ken Nakata [a], Konsei Shino [d], Hideki Yoshikawa [a], Norimasa Nakamura [e,f,*]

[a] Department of Orthopaedics, Osaka University Graduate School of Medicine, 2-2 Yamadaoka, Suita City, Osaka 565-0871, Japan
[b] Biomechanics Laboratory, Department of Mechanical Engineering, Kogakuin University, 2665-1 Nakanomachi, Hachioji City, Tokyo 192-0015, Japan
[c] McCaig Institute for Bone & Joint Health, University of Calgary, 3330 Hospital Drive Northwest, Calgary, Alberta T2N 4N1, Canada
[d] Faculty of Comprehensive Rehabilitation, Osaka Prefecture University, 3-7-30 Habikino, Habikino City, Osaka 583-8555, Japan
[e] Department of Rehabilitation Science, Osaka Health Science University, 1-9-27 Tenma, Kita-ku, Osaka City, Osaka 530-0043, Japan
[f] Center for Advanced Medical Engineering and Informatics, Osaka University, 2-2 Yamadaoka, Suita City, Osaka 565-0871, Japan

ARTICLE INFO

Article history:
Received 23 May 2010
Accepted 4 July 2010
Available online 31 July 2010

Keywords:
Mesenchymal stem cell
Cartilage tissue engineering
Allogenic cell
Aging
Animal model

ABSTRACT

One of the potential factors that may affect the results of mesenchymal stem cell (MSC)-based therapy is the age of donors and recipients. However, there have been no controlled studies to investigate the influence of skeletal maturity on the MSC-based repair of cartilage. The purpose of this study was to compare the repair quality of damaged articular cartilage treated by a scaffold-free three-dimensional tissue-engineered construct (TEC) derived from synovial MSCs between immature and mature pigs. Synovial MSCs were isolated from immature and mature pigs and the proliferation and chondrogenic differentiation capacities were compared. The TEC derived from the synovial MSCs were then implanted into equivalent chondral defects in the medial femoral condyle of both immature and mature pigs, respectively. The implanted defects were morphologically and biomechanically evaluated at 6 months postoperatively. There was no skeletal maturity-dependent difference in proliferation or chondrogenic differentiation capacity of the porcine synovial MSCs. The TEC derived from synovial MSCs promoted the repair of chondral lesion in both immature and mature pigs without the evidence of immune reaction. The repaired tissue by the TEC also exhibited similar viscoelastic properties to normal cartilage regardless of the skeletal maturity. The results of the present study not only suggest the feasibility of allogenic MSC-based cartilage repair over generations but also may validate the use of immature porcine model as clinically relevant to test the feasibility of synovial MSC-based therapies in chondral lesions.

1. Introduction

It is widely accepted that chondral injury does not usually heal spontaneously due to its avascular surroundings and unique matrix organization. Therefore, a variety of approaches have been assessed to improve cartilage healing [1,2]. Among them, chondrocyte-based therapies have been extensively studied since the reports of successful autologous chondrocyte implantation [3–8]. However, this procedure is likely to have some limitations including the sacrifice of undamaged cartilage within the same joint and alterations of chondrogenic phenotype associated with the *in vitro* expansion of the cells. Furthermore, due to alterations and degenerative changes in cartilage accompanying aging, the availability of such cells may be limited in elderly individuals [7,9].

To overcome such potential problems, stem cell therapies have been tested to facilitate regenerative tissue repair. Mesenchymal stem cells (MSCs) have the capability to differentiate into a variety of connective tissue cells including bone, cartilage, tendon, muscle, and adipose tissue [10]. These cells may be isolated from various tissues such as bone marrow, skeletal muscle, synovial membrane, adipose tissue, and umbilical cord blood [10–15]. MSCs isolated from synovial membrane may be well suited for cell-based therapies for cartilage based on the relative ease of their harvest and their strong capability of chondrogenic differentiation [11,14,16]. Recent implantation studies have reported successful cartilage repair using synovial membrane-derived MSCs [12,15,17].

* Corresponding author. Department of Rehabilitation Science, Osaka Health Science University, 1-9-27 Tenma, Kita-ku, Osaka City, Osaka 530-0043, Japan. Tel.: +81 6 6352 0093; fax: +81 6 6352 9559.
E-mail address: n-nakamura@ort.med.osaka-u.ac.jp (N. Nakamura).

0142-9612/$ – see front matter © 2010 Elsevier Ltd. All rights reserved.
doi:10.1016/j.biomaterials.2010.07.017

One of the crucial factors that may affect the results of cell-based therapies is the age of the donors and recipients. Specifically, the results of implantation surgery could be potentially affected by both the characteristics of the cells and the local environment in the lesions following implantation. Therefore, it is important to elucidate the influence of skeletal maturity on these two factors. Regarding the cell proliferation and differentiation capacities of MSCs, it is controversial as to whether they are age-dependent [18–21] or not [10,22–25]. In terms of the host tissue reaction, natural healing responses of osteochondral defects has been compared between immature and mature animals using rabbit models, and in this species the studies demonstrated better healing responses in immature animals [26–29].

On the other hand, there have been no studies which compared the results of cell-based repair of chondral defects between immature and mature animal models. Regarding the clinically relevant animal models for cartilage repair, it is difficult to create a chondral injury which does not breach the subchondral bone in small animals such as rabbits, rats and mice due to the limited thickness of their articular cartilage. Therefore, in consideration of clinical relevance, it is preferable to utilize a large animal model to investigate the influence of maturity on the results of cell-based therapy in chondral lesions.

As a potential MSC-based therapeutic method, we have developed a scaffold-free three-dimensional tissue-engineered construct (TEC) composed of allogenic mesenchymal stem cells (MSCs) derived from the synovium and extracellular matrices (ECMs) synthesized by the cells [11], and demonstrated the feasibility of the resultant TEC to facilitate cartilage repair in a large animal study [12]. The TEC efficiently repaired the chondral defects by developing a cartilage-like tissue without the development of any immunologic reaction [12]. A potential limitation of this previous study was the use of an immature animal model (cell donors and recipients) and a concern that the successful chondrogenic repair without immunologic reaction *in vivo* might have been due to the immaturity of the recipient animals which may be a growth-oriented environment.

In the present study, we used both skeletally immature and mature animals as recipients, and compared the results of TEC implantation to the chondral lesions morphologically and biomechanically in order to elucidate the influence of the skeletally maturity on subsequent cartilage repair with the TEC.

2. Materials and methods

All procedures of this study followed the Declaration of Helsinki principles.

2.1. Harvest of synovial tissue and isolation of the cells

Porcine synovial membranes were obtained aseptically from the knee joints of immature (3–4 months of age) ($N = 3$) or mature (12 months of age) ($N = 3$) male pigs within 12 h of death. The cell isolation protocol was essentially that used previously for the isolation of human synovial derived MSC [11]. Briefly, synovial membrane specimens were rinsed with phosphate buffered saline (PBS), minced meticulously, and digested with 0.1% collagenase IV (Sigma, St. Louis, MO, USA) for 1.5 h at 37 °C. After neutralization of the collagenase with growth medium containing high-glucose Dulbecco's modified Eagle's medium (HG-DMEM; Gibco BRL, Life Technologies Inc., Rockville, MD, USA) supplemented with 10% fetal bovine serum (FBS; HyClone, Logan, UT, USA) and 1% penicillin/streptomycin (Gibco BRL, Life Technologies Inc.), the cells were collected by centrifugation, washed with PBS, resuspended in growth medium, and plated in culture dishes. The characteristics of the porcine cells were similar to those of the human synovium derived MSC with regard to morphology, growth characteristics and multipotent differentiation capacity (to osteogenic, chondrogenic and adipogenic lineages) [11,12,30]. For expansion, cells were cultured in the growth medium at 37 °C in a humidified atmosphere of 5% CO_2. The medium was replaced once per week. After 15–28 days of primary culture, when the cells reached confluence, they were washed twice with PBS, harvested by treatment with trypsin-EDTA (0.25% trypsin and 1 mM EDTA: Gibco BRL, Life Technologies Inc.), and replated at 1:3 dilutions for the first subculture. Cell passages were continued in the same manner with 1:3 dilutions when cultures reached near confluence. Cells at passages 4–7 were used in the present studies.

2.2. Cell proliferation assay

To assess cell proliferation between cells derived from immature and mature animals, cell counts and WST-1 assays [31,32] were performed at day 1, 3, 7, 10 and 14 of culture. The cells were isolated by trypsinization, washed extensively, and then replated at a density of 5×10^3 cells/cm^2 in 6-well and 96-well culture plates for cell counts and WST-1 assays, respectively. MSCs were cultured in growth medium and the medium was replaced twice per week. Subsequently, the numbers of cells were counted at each measurement day using a hemocytometer. In addition, 10 μl of Premix WST-1 solution (TAKARA Bio, Shiga, Japan) and 100 μl of medium were added to the cell monolayers in the 96-well plates and these were then incubated at 37 °C for an additional 2 h. Supernatants were quantified spectrophotometrically at 440 nm with reference wavelength at 620 nm. Results were reported as optical density (OD) units.

2.3. In vitro chondrogenesis

To assess chondrogenic differentiation, a pellet culture system was used [33]. Approximately 2×10^5 cells were placed in a 15-ml polypropylene tube, and centrifuged at 500 g for 10 min. The pellets were cultured at 37 °C with 5% CO_2 in 500 μl of chondrogenic culture medium that contained HG-DMEM supplemented with 50 mg/ml ascorbate-2-phosphate, 100 mg/ml sodium pyruvate, and 50 mg/ml insulin, transferrin, selenious acid (ITS) + Premix (BD Biosciences, California, USA), and 200 ng/ml recombinant human bone morphogenetic protein 2 (rhBMP2) (a generous gift from Wyeth, Massachusetts, USA) as described previously [30,34]. The optimal concentration of rhBMP2 was determined from preliminary *in vitro* optimization studies on chondrogenic differentiation of MSCs in pellet cultures (data not shown). The medium was replaced twice per week for 3 weeks.

2.4. Reverse transcription-polymerase chain reaction (RT-PCR)

Total RNAs from the pellets were extracted using a RNeasy Mini Kit (Qiagen, Valencia, CA, USA). Complementary DNAs (cDNAs) were obtained by RT of 1 μg total RNA using a Reverse Transcription System (Promega, San Luis Obispo, CA, USA) with random primers. Equal amounts of each RT product were amplified by PCR with TaKaRa Ex Taq (TAKARA Bio, Shiga, Japan). PCR reactions were carried out in iCyclerTM (BioRad Laboratories, Hercules, CA, USA). After initial denaturation at 94 °C for 5 min, PCR involved amplification cycles of 30 s at 94 °C, 30 s at 60 °C, and 30 s at 72 °C, followed by elongation for 7 min at 72 °C. PCR primers used were as follows: pig-GAPDH (forward): CTG CCC CTT CTG CTG ATG C, (reverse): CAT CAC GCC ACA GTT TCC CA, pig-collagen 2a1 (forward): ATT GTA GGA CCC AAA GGA CCT C, (reverse): GGT CCC AGG TTC TCC ATC TC. PCR products were separated on 2% agarose gel containing ethidium bromide and evaluated for the expression of mRNA for each gene. The band intensities were captured into a computer with a digital image scanner, quantified using imageJ (NIH, Bethesda, MD) and subjected to statistical analyses.

2.5. Histological assessment of the pellets

The cell pellet cultures were fixed in 4% paraformaldehyde, rinsed twice with PBS, embedded in paraffin, cut into 5 μm sections, and then stained for 2 h at room temperature with 1% Alcian blue (Alcian Blue 8 GX; Sigma, Missouri, USA) in 0.1N HCl, and subsequently counter stained with Kernechtrot.

2.6. Measurement of glycosaminoglycan (GAG) levels

Proteoglycan levels in the pellets were measured by a color method as described previously [35], with minor modification. Briefly, synovial cell pellets were digested for 4 h at 65 °C with a papain solution (Sigma, St. Louis, MO, USA). Samples from the papain digest were subsequently assayed for GAG as a measure of proteoglycan content. GAGs were assayed using the 1,9-dimethylmethylene blue binding (DMMB) assay, using a chondroitin sulfate standard curve (Nacalai Tesque, Kyoto, Japan).

2.7. Development of the TECs

Synovial MSCs were plated on culture dishes at a density of 4.0×10^5 cells/cm^2 in growth medium containing 0.2 mM ascorbate-2-phosphate (Asc-2P), an optimal concentration from earlier studies [11,12]. Within a day, the cells became confluent. After an additional 7–14 days in culture, a complex of the cultured cells and the ECM synthesized by the cells was detached from the substratum by application of shear stress using gentle pipetting. The detached monolayer complex was left in suspension to form a three-dimensional structure by active tissue contraction. This tissue was termed a basic scaffold-free three-dimensional TEC.

2.8. Implantation of the TEC to chondral defects

As previously reported [12], porcine MSCs (4.0×10^5 cells/cm^2) derived from immature animals (3–4 months of age) were cultured with Asc-2P in 6 cm

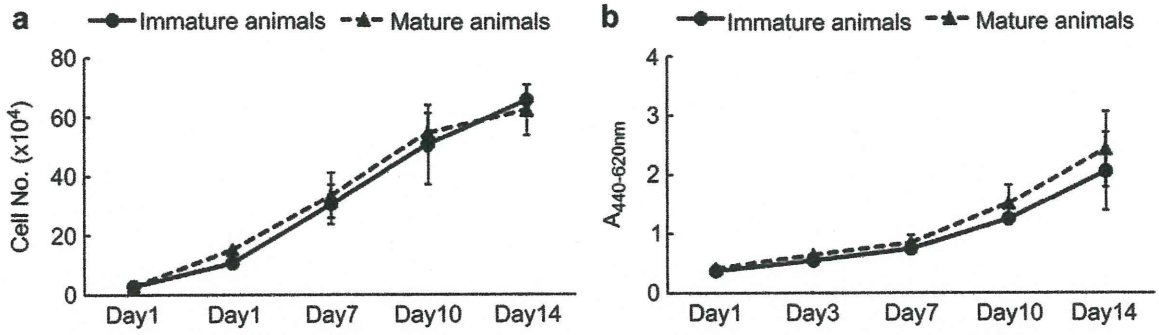

Fig. 1. Cell Proliferation assay assessed by cell counting (a) and the WST-1 method (b). There are no significant differences in proliferative capacity between immature ($N = 3$) and mature porcine synovial MSCs ($N = 3$).

diameter culture dishes (21.3 cm^2) for 7 days, and the resultant TECs were prepared as an allograft without any chondrogenic stimulation. 6 immature (4-month-old) pigs and 7 skeletally mature (12-month-old) pigs were anesthetized by intramuscular injection of a mixture of ketamine hydrochloride (50 mg/ml and 0.6 ml/kg of body weight) and xylazine (20 mg/ml and 0.3 ml/kg of body weight) and continuous intravenous injection of propofol (10 mg/ml and 8 ml/kg/h). After a medial parapatella incision, the medial femoral condyles of the both knees were exposed with the knee in deep flexion, and chondral defects of 8.5 mm diameter and 2.0 mm depth which did not breach the subchondral bone were created on the medial femoral condyle using an electric router (Proxxon, Niersbach, Germany) and diamond disc grinding (Shofu Inc., Kyoto, Japan). The TEC were then implanted into the defects without suture for 8 knees in the immature pigs and 6 knees of the mature pigs. In the control groups, the defect was left empty for 4 knees of the immature pigs and 6 knees of the mature pigs. All animals were immobilized for 7 days, and euthanized under anesthesia at 6 months after surgery. Each graft site was divided into two parts. One was fixed and used for subsequent paraffin sectioning and histological analysis, and the other was subjected to mechanical compression tests.

2.9. Macroscopic and histological evaluation

The macroscopic findings were assessed in accordance with the following criteria; the score 2 was complete resurface (>90% coverage), 1 was partial resurface (50–90% coverage), and 0 was poor resurface (<50% coverage) [12].

For histological evaluation, tissue was fixed with 4% paraformaldehyde in phosphate buffer (pH 7.4), decalcified with EDTA, embedded in paraffin, and 4 μm sections were prepared. The sections were stained with HE or Safranin O.

The histology of repair tissue at 6 months was evaluated by the modified International Cartilage Repair Society (ICRS) Visual Histological Assessment Scale [36]. As this original scale is usually applied to human biopsy specimens of 2 mm diameter and not to large animal specimens, the repair tissue was divided into 4 parts of 2 mm width and each area was evaluated by the ICRS Visual Histological Assessment Scale. Moreover, a new criteria category "Integration" was implemented. Good integration was a score of 3, and poor or no integration a score of 0. This criterion was utilized for both sides of a divided area [12]. All scores for each area were averaged.

2.10. Mechanical testing

Unconfined compression tests were performed for normal cartilage and the repair tissue in defects treated with or without TEC as previously reported [12]. A cylindrical-shaped cartilage-subchondral bone specimen of 4 mm diameter and 5–8 mm depth was taken in the medial condyle of the femur. The specimen was placed on a permeable stage soaked in saline solution at 37 °C. Compressive deformation was generated using a linear actuator (LAH-46-3002-F-SP, Harmonic Drive Systems, Tokyo, Japan) with the position repeatability of 0.5 mm under 50N of axial force. Compressive loads were measured with a custom-made ring-shaped load transducer with strain gauges having the rated output of 1.76N and

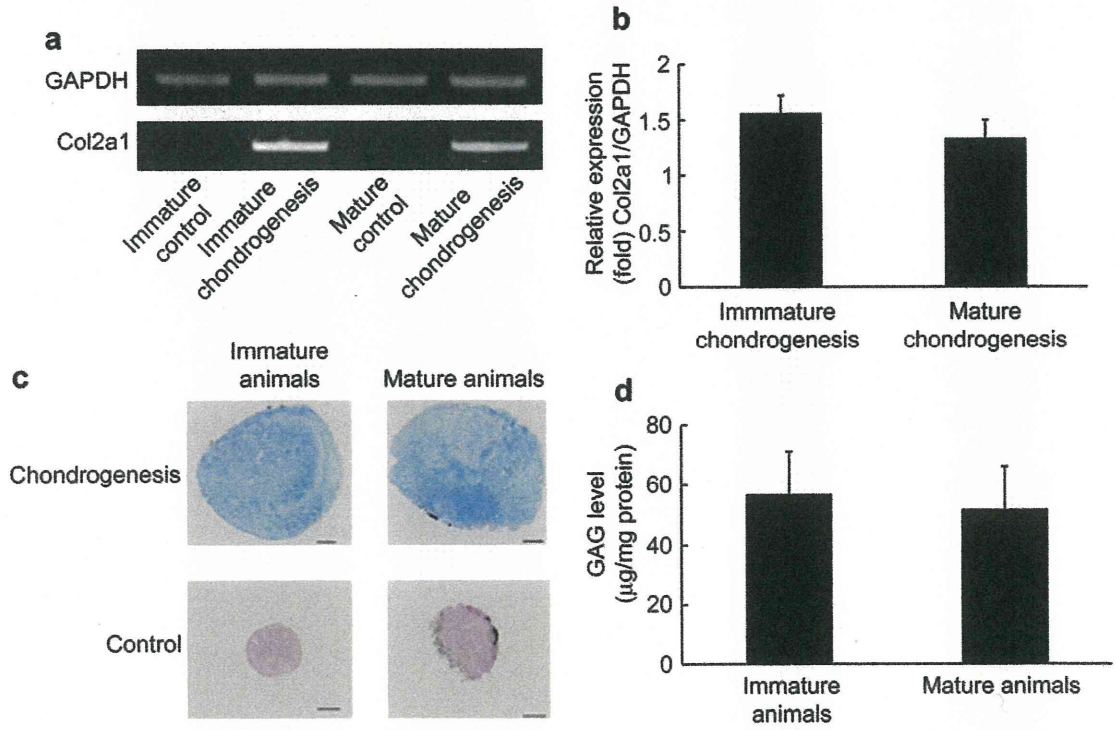

Fig. 2. Chondrogenic potential of porcine MSCs derived from immature and mature animals assessed by collagen II expression by RT-PCR (a, b), alcian blue staing (c), and GAG synthesis (d). Bar = 200 μm. There are no significant differences detected between immature-pellets ($N = 3$) and mature-pellets ($N = 3$) in RT-PCR (b) and GAG synthesis (d).

a non-linearity of 0.01%, while compressive deformation in cartilage was measured from the actuator displacement assuming no deformation in the subchondral bone. Compressive loads were divided by the cross-sectional area of each specimen to obtain nominal stress values. After the width of the repair tissue was measured with a digital microscope (VHX-100, Keyence), the deformation of cartilage was transformed to strain. Finally, the stress–strain relationship of the repair tissue was obtained.

2.11. Statistical analysis

The results are presented as mean ± SD. The results of the experiments were analyzed by Mann–Whitney *U* test using JMP 7 (SAS Institute, Cary, NC, USA) and significance was set at $p < 0.05$.

3. Results

3.1. Cell proliferation and chondrogenic differentiation capacity of immature and mature porcine synovial MSCs

Cell number assessments, as well as WST-1 assays demonstrated that there were no significant differences in the proliferation capacity of porcine synovial MSCs derived from immature or mature animals (Fig. 1a, b). To evaluate the chondrogenic differentiation potential, semiquantitative analyses were performed using a pellet culture system. There were no significant differences in expression level of collagen II detected by RT-PCR between the pellets from immature animals versus those from mature animals ($p = 0.2752$) (Fig. 2a, b). Based on Alcian blue staining of the cell pellets, increases in staining were prominent in the center area of pellets from both immature and mature animals (Fig. 2c). Likewise, there were no significant differences in GAG synthesis noted between the chondrogenic pellets from the immature (56.9 ± 14.3 μg/mg protein) and mature donor age groups (51.8 ± 14.4 μg/mg protein) ($p = 0.5127$) (Fig. 2d).

These results suggested that maturity may not significantly affect the chondrogenic differentiation capacity of porcine synovial MSCs and based on the results, we decided to use immature MSCs consistently as the source of the TEC for the following implantation studies.

3.2. Macroscopic and histological evaluation of repaired cartilage

At 6 months post-implantation, regardless of skeletal maturity, untreated lesions had no or only partial tissue coverage (Fig. 3a, c), while the defects treated with the TEC were totally or partially covered with repaired tissue (Fig. 3b, d). The mean macroscopic score for the TEC group (1.50 ± 0.50, immature group, and 1.50 ± 0.50, mature group) was significantly higher than that for the untreated group (0.25 ± 0.50, immature group, and 0.67 ± 0.75, mature group) ($p = 0.017$, and $p = 0.034$, respectively) (Fig. 3e).

Histologically, the chondral lesions in the untreated control groups (defects only) showed evidence of osteoarthritic changes with loss of cartilage and erosion of subchondral bone in both skeletally immature and mature recipients (Fig. 4a, b). Conversely, when implanted with a TEC, the defects were repaired with a chondrogenic-like tissue with positive Safranin O staining, regardless of skeletal maturity (Fig. 4c, d). Higher magnification views showed that there was good tissue integration to the

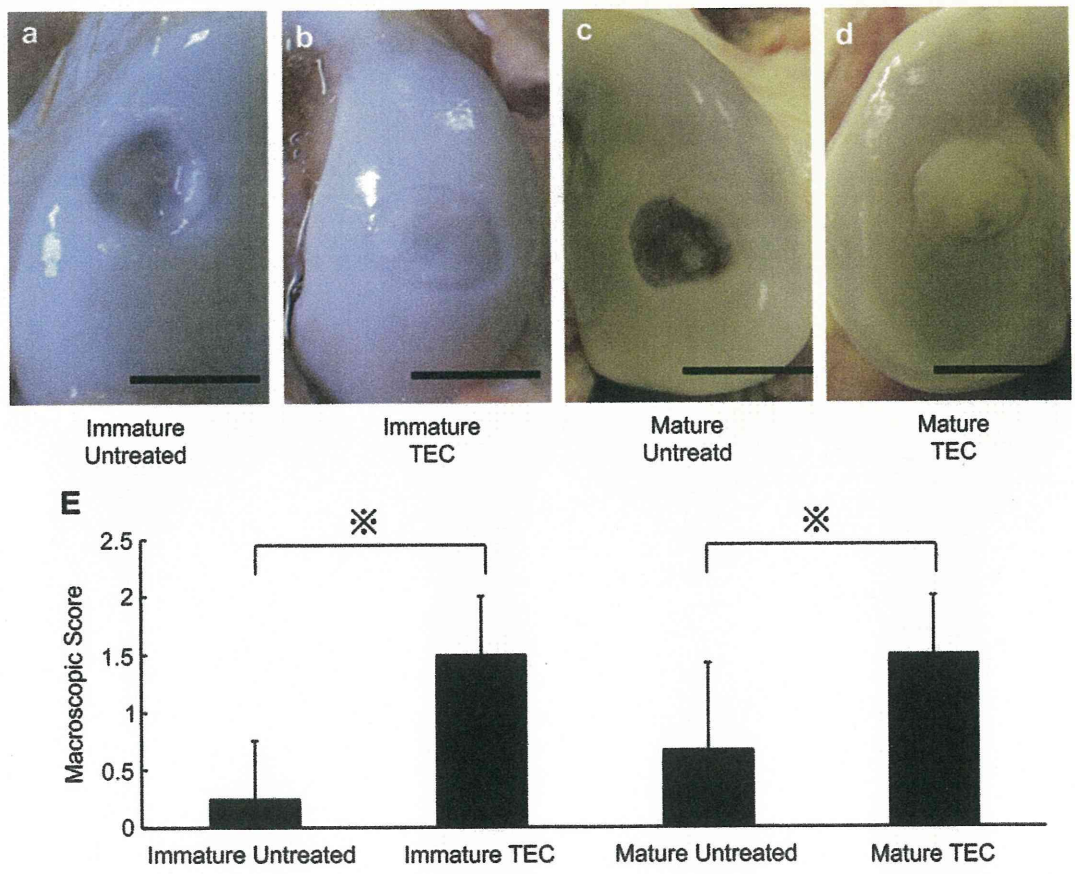

Fig. 3. Macroscopic view of immature (a, b) or mature (c, d) porcine chondral lesion treated without (a, c) or with the TEC (b, d) at 6 months after operation. Bar = 10 mm. (e) Macroscopic score of the chondral lesion treated with the TEC (Immature recipients, $N = 8$, Mature recipients, $N = 6$) or untreated (Immature recipients, $N = 4$, Mature recipients, $N = 6$) at 6 months. Regardless of skeletal maturity, the TEC group shows significantly higher score than the untreated group. ※; $p < 0.05$.

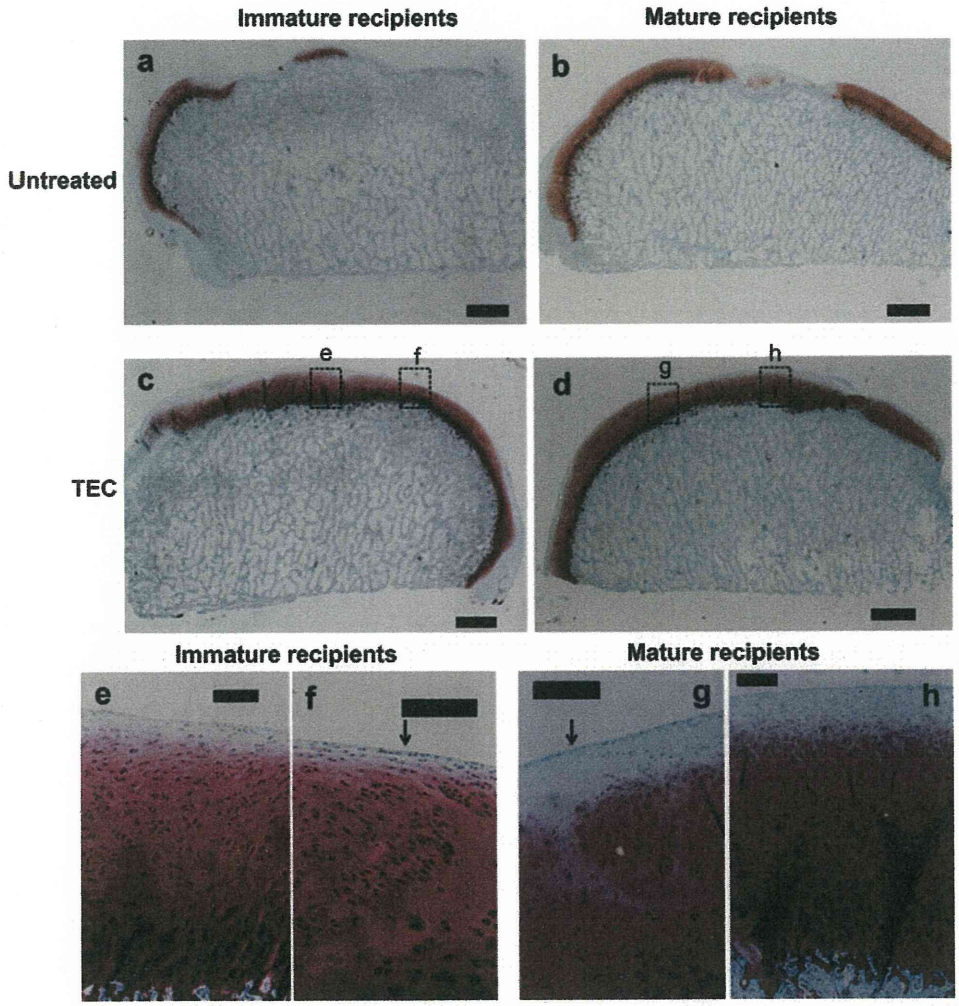

Fig. 4. Safranin O staining of untreated chondral lesions (a, b) or lesions repaired by the TEC (c, d). (a, c) immature recipients. (b, d) mature recipients. Bar = 1 mm. Higher magnification view at the margin (f, g) and center (e, h) area of the repaired tissue by the TEC. Bar = 200 μm. Regardless of the maturity, the defects treated with the TEC are completely filled with Safranin O positive repaired tissue (c, d) with good tissue integration (f, g, arrow). There is scarce healing response observed the untreated control group with bony erosion (a, b).

adjacent cartilage obtained when the TEC were implanted in both immature and mature recipients (Fig. 4f, g, arrows). The repair tissue exhibited predominantly spindle-shaped fibroblast-like cells in the superficial area of the repair tissue, while the majority of the remaining repair matrix contained round-shaped cells in lacuna (Fig. 4e, h). Following implantation, no histological findings were obtained that suggested either central necrosis of the implanted TEC or that an abnormal inflammatory macrophage and lymphocyte response consistent with immunological rejection had occurred in this allogenic situation, regardless of skeletal maturity.

Based on the modified ICRS histological scoring, the TEC group exhibited significantly higher scores than did the control group in all criteria categories in the immature recipients (Fig. 5a). In mature recipients, the TEC group had significantly higher scores than did the corresponding control group in all categories except the "Matrix" and "Cell distribution" categories (Fig. 5b). Comparing the repair tissues by the TEC in immature and mature recipients, there was no significant difference detected (Fig. 5c).

3.3. Mechanical properties of repaired tissue

Using the methods as previously reported, we evaluated the mechanical properties of the TEC-mediated repair tissue at two different compression speeds for the compression tests [12,37]. Namely, the viscoelasticity of cartilage which retains interstitial water would be mainly reflected by faster compression test (at 100 μm/s) outcomes, while the matrix viscoelasticity without interstitial water retention would be mainly reflected by slower compression test (at 4 μm/s) outcomes.

In the tissue localized in the defects of the untreated control group, the tangent modulus (defined as the slope of the curve at 5% of strain) in immature recipients was significantly lower than that for normal cartilage at a compression rate of either 4 μm/s (Fig. 6a, 126 ± 61 kPa versus 344 ± 217 kPa) or 100 μm/s (Fig. 6b, 174 ± 225 kPa versus 652 ± 354 kPa) ($p = 0.0188$ at 4 μm/s, and 0.0187 at 100 μm/s, respectively). In contrast, there were no significant differences detected between the tangent modulus for the repair tissue by the TEC and that for normal cartilage at either 4 μm/s (Fig. 6a, 215 ± 93 kPa versus 344 ± 217 kPa) or 100 μm/s (Fig. 6b, 875 ± 493 kPa versus 652 ± 354 kPa) ($p = 0.2215$ at 4 μm/s, and 0.3146 at 100 μm/s, respectively) in immature recipients. Similarly, the mean tangent modulus in the untreated mature recipients (46 ± 34 kPa) was significantly lower than that for normal cartilage (173 ± 73 kPa) at a compression rate of 4 μm/s ($p = 0.0090$) (Fig. 6a), while there were no significant differences detected between the tangent modulus for repaired tissue in

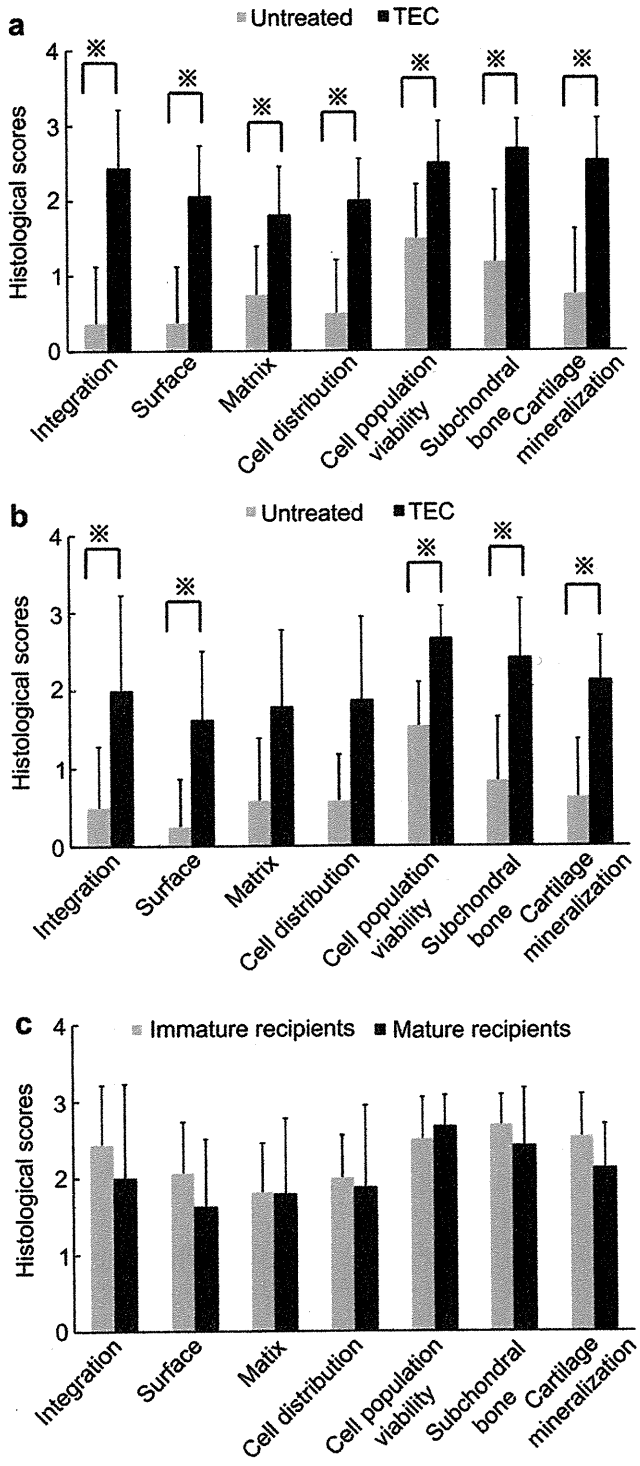

Fig. 5. Modified ICRS score in repaired cartilage immature (a) and mature recipients (b). The TEC group ($N = 8$) exhibits significantly higher scores than does the untreated control group ($N = 4$) in all the criteria categories in the immature recipients. ※; $p < 0.05$. Likewise, the TEC group ($N = 6$) exhibits significantly higher scores than does the untreated control group ($N = 6$) in the criteria categories except for the "Matrix" and "Cell distribution" categories in the mature recipients. ※; $p < 0.05$. (c) As to the quality of repaired cartilage by the TEC, there is no significant difference observed in any criteria category between the immature ($N = 8$) and mature recipients ($N = 6$).

mature recipients treated by the TEC and that for normal cartilage at either 4 μm/s (Fig. 6a, 123 ± 77 kPa versus 173 ± 73 kPa) or 100 μm/s (Fig. 6b, 293 ± 268 kPa versus 457 ± 212 kPa) ($p = 0.3472$ at 4 μm/s, and 0.2506 at 100 μm/s, respectively). These results suggest that the viscoelastic properties of the tissue in defects repaired by the TEC are likely similar to those of normal cartilage, regardless of skeletal maturity.

4. Discussion

Recent animal and clinical studies suggested the feasibility of MSC-based therapies in cartilage repair [38–44]. Most of the procedures utilized scaffolds to provide three-dimensional environment to stem cells. Scaffolds generally contain synthetic polymers or biological materials and there are still several concerns associated with the long-term safety of these materials. In order to avoid unknown risk, such materials should ideally be excluded throughout the treatment procedure, and in this regard, a scaffold-free cell delivery system could be an excellent alternative. With this concept, we have developed the scaffold-free tissue-engineered construct (TEC) derived from allogenic synovial MSCs [11,12]. In addition to the potentially safety as a surgical implant, the TEC has been shown to have the feasibility to facilitate cartilage repair [12] which is comparable with other scaffold-based MSC therapies [38–44] and thus could be a promising option among various cell-based therapies in chondral lesions.

It is notable that the TEC is derived of allogenic synovial MSCs and that the results in the present study demonstrated that the TEC effectively promote cartilage repair without the development of any immunologic reaction in a large animal study [12]. It is fairly widely accepted that MSCs exhibit immune-tolerance capacity [45–47] and the availability of allogenic MSCs to repair chondral lesions has been also reported in an animal study [43]. Taken together, it is suggested that allogenic MSC-based therapies are feasible to cartilage repair. Regarding the donor cells, it has been controversial as to whether the cell proliferation and differentiation capacities of MSCs derived from different tissue sources exhibit age-dependency [10,18–25]. The present study demonstrated that there were no significant differences in these capacities between cells from immature and mature porcine synovial membranes. A previous study likewise showed that the *in vitro* expandability and differentiation capacity of human synovial MSCs also are not overtly influenced by donor age [10]. Such similarity among these two species suggests that age-independency in the proliferation and differentiation capacity could be characteristics specific to synovial MSCs. Taken together, synovial MSCs could be obtained from donors of variety of ages for allogenic cell-based therapies in cartilage repair.

On the other hand, several studies have shown that the natural healing response of rabbits to osteochondral defects was better in immature animals than in mature animals [26–29]. Therefore, although there have been no studies demonstrating an age-dependent repair response of cartilage in a large animal model, skeletal maturity might be likewise an important variable the repair and differentiation process following stem cell-based therapies in such larger species. The results of the present study demonstrated that TEC implantation into porcine chondral defects effectively contributed to chondrogenic repair, with good tissue integration to the adjacent cartilage tissue. The repair tissue exhibited viscoelastic properties similar to normal cartilage. Notably, such repair responses were equivalently observed in both immature and mature recipients. In addition, there were no abnormal inflammatory responses detected, observations which might be suggestive of immunological rejection, in either immature or mature animal recipients. These results suggest that an

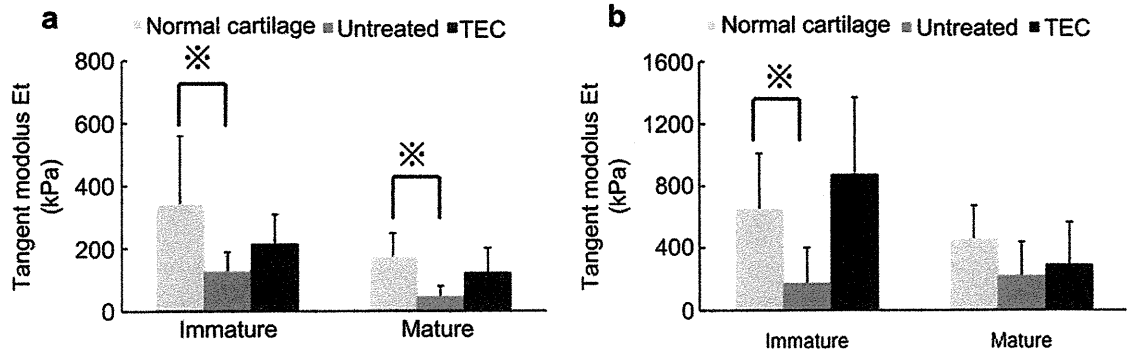

Fig. 6. The results of compression tests at slower compression speed (4 μm/s) (a) and at faster compression speed (100 μm/s) (b). (Immature recipients: normal cartilage, $N = 11$, TEC, $N = 7$, untreated, $N = 4$, Mature recipients: normal cartilage, $N = 5$, TEC, $N = 5$, untreated, $N = 5$) Regardless of skeletal maturity, there is no significant difference detected in the tangent modulus of the repaired tissue by the TEC and of normal cartilage at either slower or faster compression speed. Conversely, untreated cartilage, whether immature or mature, showed significantly lower tangent modulus than normal cartilage at either slower or faster compression speed. ※; $p < 0.05$.

immunological reaction subsequent to the implantation of allogenic MSC-based materials may be negligible regardless of maturity. In interpreting the results on the present study, it should be taken into account that the injury model we used was chondral injury model which did not breach the subchondral bone. Such injury accompanies minimal bleeding response and such unique repair environment might have led to the converse results from previous natural healing studies with osteochondral injury model which accompanied extensive bleeding [26–29].

Taken together, the skeletal maturity of recipient animal does not likely influence the repair quality of allogenic MSC-treated chondral lesions and the results of the present study suggest the feasibility of the synovial MSC-based therapies to chondral lesions in both adolescent and adult cases, which could increase the opportunity of clinical applications in the future. Furthermore, equivalent cartilage repair response observed in immature and mature recipients coupled with similar chondrogenic differentiation capacity in immature and mature MSCs suggest the validity of the use of immature porcine animal models to test the feasibility of synovial MSC-based therapies, whether allogenic or autologous, in chondral lesions. The use of skeletally mature large animals specifically requires large expense and thus the present results could contribute to the valid cost reduction in future experimental preclinical studies.

As a potential limitation of the present study, are we did not perform detailed laboratory investigations to detect specific immunologic reactions such as development of antibodies or cell-mediated responses. Additionally, we did not follow the implantation surgery beyond 6 months. Longer follow-up studies with laboratory experiments would be required towards clinical applications. However, the histological analyses in the present study revealed that the chondrogenic repair responses as well as the lack in immunologic reactions was very consistent by 6 months post-implantation, and the limitations do not likely affect the major conclusions drawn from the findings.

5. Conclusion

The TEC, allogenic MSC-based approach was proved to be feasible to cartilage repair regardless of the skeletal maturity. The use of allogenic stem cells could be advantageous from a time- and cost-saving perspective, without tissue sacrifice of host tissue in comparison with autologous cell-based approach. Therefore the results of the present studies would support the clinical application of this strategy to promote cartilage repair and regeneration in patients over wide range of patient ages. This may be particularly relevant to older patients where autologous chondrocytes are limited in number and quality.

Acknowledgement

This study was supported by a grant from the New Energy and Industrial Technology Development Organization, Japan, and Grant-in-Aid for Scientific Research (B), Japan Society for the promotion of Science, Japan. DAH is the Calgary Foundation-Grace Glaum Professor in Arthritis Research and supported by grants from the Canadian Arthritis Network and an AHFMR Team Grant in Osteoarthritis.

References

[1] Buckwalter JA. Articular cartilage injuries. Clin Orthop Relat Res 2002;402:21–37.
[2] Hunziker EB. Articular cartilage repair: basic science and clinical progress. A review of the current status and prospects. Osteoarthr Cartil 2002;10:432–63.
[3] Brittberg M, Peterson L, Sjogren-Jansson E, Tallheden T, Lindahl A. Articular cartilage engineering with autologous chondrocyte transplantation. a review of recent developments. J Bone Jt Surg Am 2003;85-A(Suppl. 3):109–15.
[4] Ochi M, Adachi N, Nobuto H, Yanada S, Ito Y, Agung M. Articular cartilage repair using tissue engineering technique–novel approach with minimally invasive procedure. Artif Organs 2004;28:28–32.
[5] Marcacci M, Berruto M, Brocchetta D, Delcogliano A, Ghinelli D, Gobbi A, et al. Articular cartilage engineering with Hyalograft C: 3-year clinical results. Clin Orthop Relat Res 2005;435:96–105.
[6] Chajra H, Rousseau CF, Cortial D, Ronziere MC, Herbage D, Mallein-Gerin F, et al. Collagen-based biomaterials and cartilage engineering. application to osteochondral defects. Biomed Mater Eng 2008;18:S33–45.
[7] Iwasa J, Engebretsen L, Shima Y, Ochi M. Clinical application of scaffolds for cartilage tissue engineering. Knee Surg Sports Traumatol Arthrosc 2009;17:561–77.
[8] Safran MR, Kim H, Zaffagnini S. The use of scaffolds in the management of articular cartilage injury. J Am Acad Orthop Surg 2008;16:306–11.
[9] Nehrer S, Domayer S, Dorotka R, Schatz K, Bindreiter U, Kotz R. Three-year clinical outcome after chondrocyte transplantation using a hyaluronan matrix for cartilage repair. Eur J Radiol 2006;57:3–8.
[10] De Bari C, Dell'Accio F, Tylzanowski P, Luyten FP. Multipotent mesenchymal stem cells from adult human synovial membrane. Arthritis Rheum 2001;44:1928–42.
[11] Ando W, Tateishi K, Katakai D, Hart DA, Higuchi C, Nakata K, et al. In vitro generation of a scaffold-free tissue-engineered construct (TEC) derived from human synovial mesenchymal stem cells: biological and mechanical properties and further chondrogenic potential. Tissue Eng Part A 2008;14:2041–9.
[12] Ando W, Tateishi K, Hart DA, Katakai D, Tanaka Y, Nakata K, et al. Cartilage repair using an in vitro generated scaffold-free tissue-engineered construct derived from porcine synovial mesenchymal stem cells. Biomaterials 2007;28:5462–70.
[13] Martin MJ, Muotri A, Gage F, Varki A. Human embryonic stem cells express an immunogenic nonhuman sialic acid. Nat Med 2005;11:228–32.
[14] Sakaguchi Y, Sekiya I, Yagishita K, Muneta T. Comparison of human stem cells derived from various mesenchymal tissues: superiority of synovium as a cell source. Arthritis Rheum 2005;52:2521–9.

[15] Koga H, Engebretsen L, Brinchmann JE, Muneta T, Sekiya I. Mesenchymal stem cell-based therapy for cartilage repair: a review. Knee Surg Sports Traumatol Arthrosc 2009;17:1289–97.
[16] Segawa Y, Muneta T, Makino H, Nimura A, Mochizuki T, Ju YJ, et al. Mesenchymal stem cells derived from synovium, meniscus, anterior cruciate ligament, and articular chondrocytes share similar gene expression profiles. J Orthop Res 2009;27:435–41.
[17] Koga H, Shimaya M, Muneta T, Nimura A, Morito T, Hayashi M, et al. Local adherent technique for transplanting mesenchymal stem cells as a potential treatment of cartilage defect. Arthritis Res Ther 2008;10:R84.
[18] Murphy JM, Dixon K, Beck S, Fabian D, Feldman A, Barry F. Reduced chondrogenic and adipogenic activity of mesenchymal stem cells from patients with advanced osteoarthritis. Arthritis Rheum 2002;46:704–13.
[19] Quarto R, Thomas D, Liang CT. Bone progenitor cell deficits and the age-associated decline in bone repair capacity. Calcif Tissue Int 1995;56:123–9.
[20] Bergman RJ, Gazit D, Kahn AJ, Gruber H, McDougall S, Hahn TJ. Age-related changes in osteogenic stem cells in mice. J Bone Miner Res 1996;11:568–77.
[21] Kretlow JD, Jin YQ, Liu W, Zhang WJ, Hong TH, Zhou G, et al. Donor age and cell passage affects differentiation potential of murine bone marrow-derived stem cells. BMC Cell Biol 2008;9:60.
[22] Oreffo RO, Bennett A, Carr AJ, Triffitt JT. Patients with primary osteoarthritis show no change with ageing in the number of osteogenic precursors. Scand J Rheumatol 1998;27:415–24.
[23] Leskela HV, Risteli J, Niskanen S, Koivunen J, Ivaska KK, Lehenkari P. Osteoblast recruitment from stem cells does not decrease by age at late adulthood. Biochem Biophys Res Commun 2003;311:1008–13.
[24] De Bari C, Dell'Accio F, Luyten FP. Human periosteum-derived cells maintain phenotypic stability and chondrogenic potential throughout expansion regardless of donor age. Arthritis Rheum 2001;44:85–95.
[25] Scharstuhl A, Schewe B, Benz K, Gaissmaier C, Buhring HJ, Stoop R. Chondrogenic potential of human adult mesenchymal stem cells is independent of age or osteoarthritis etiology. Stem Cells 2007;25:3244–51.
[26] Rudert M. Histological evaluation of osteochondral defects: consideration of animal models with emphasis on the rabbit, experimental setup, follow-up and applied methods. Cells Tissues Organs 2002;171:229–40.
[27] Bos PK, Verhaar JA, van Osch GJ. Age-related differences in articular cartilage wound healing: a potential role for transforming growth factor beta1 in adult cartilage repair. Adv Exp Med Biol 2006;585:297–309.
[28] Yamamoto T, Wakitani S, Imoto K, Hattori T, Nakaya H, Saito M, et al. Fibroblast growth factor-2 promotes the repair of partial thickness defects of articular cartilage in immature rabbits but not in mature rabbits. Osteoarthr Cartil 2004;12:636–41.
[29] Wei X, Gao J, Messner K. Maturation-dependent repair of untreated osteochondral defects in the rabbit knee joint. J Biomed Mater Res 1997;34:63–72.
[30] Tateishi K, Higuchi C, Ando W, Nakata K, Hashimoto J, Hart DA, et al. The immunosuppressant FK506 promotes development of the chondrogenic phenotype in human synovial stromal cells via modulation of the Smad signaling pathway. Osteoarthr Cartil 2007;15:709–18.
[31] Cook JA, Mitchell JB. Viability measurements in mammalian cell systems. Anal Biochem 1989;179:1–7.
[32] Mosmann T. Rapid colorimetric assay for cellular growth and survival: application to proliferation and cytotoxicity assays. J Immunol Methods 1983;65:55–63.
[33] Johnstone B, Hering TM, Caplan AI, Goldberg VM, Yoo JU. In vitro chondrogenesis of bone marrow-derived mesenchymal progenitor cells. Exp Cell Res 1998;238:265–72.
[34] Sekiya I, Vuoristo JT, Larson BL, Prockop DJ. In vitro cartilage formation by human adult stem cells from bone marrow stroma defines the sequence of cellular and molecular events during chondrogenesis. Proc Natl Acad Sci U S A 2002;99:4397–402.
[35] Karran EH, Young TJ, Markwell RE, Harper GP. In vivo model of cartilage degradation–effects of a matrix metalloproteinase inhibitor. Ann Rheum Dis 1995;54:662–9.
[36] Mainil-Varlet P, Aigner T, Brittberg M, Bullough P, Hollander A, Hunziker E, et al. Histological assessment of cartilage repair: a report by the histology endpoint committee of the international cartilage repair society (ICRS). J Bone Jt Surg Am 2003;85-A(Suppl. 2):45–57.
[37] Huang CY, Soltz MA, Kopacz M, Mow VC, Ateshian GA. Experimental verification of the roles of intrinsic matrix viscoelasticity and tension-compression nonlinearity in the biphasic response of cartilage. J Biomech Eng 2003;125:84–93.
[38] Wang W, Li B, Li Y, Jiang Y, Ouyang H, Gao C. In vivo restoration of full-thickness cartilage defects by poly(lactide-co-glycolide) sponges filled with fibrin gel, bone marrow mesenchymal stem cells and DNA complexes. Biomaterials 2010;31:5953–65.
[39] Zscharnack M, Hepp P, Richter R, Aigner T, Schulz R, Somerson J, et al. Repair of chronic osteochondral defects using predifferentiated mesenchymal stem cells in an ovine model. Am J Sports Med in press
[40] Zheng L, Fan HS, Sun J, Chen XN, Wang G, Zhang L, et al. Chondrogenic differentiation of mesenchymal stem cells induced by collagen-based hydrogel: an in vivo study. J Biomed Mater Res A 2010;93:783–92.
[41] Jung M, Kaszap B, Redohl A, Steck E, Breusch S, Richter W, et al. Enhanced early tissue regeneration after matrix-assisted autologous mesenchymal stem cell transplantation in full thickness chondral defects in a minipig model. Cell Transpl 2009;18:923–32.
[42] Cui L, Wu Y, Cen L, Zhou H, Yin S, Liu G, et al. Repair of articular cartilage defect in non-weight bearing areas using adipose derived stem cells loaded polyglycolic acid mesh. Biomaterials 2009;30:2683–93.
[43] Nishimori M, Deie M, Kanaya A, Exham H, Adachi N, Ochi M. Repair of chronic osteochondral defects in the rat. A bone marrow-stimulating procedure enhanced by cultured allogenic bone marrow mesenchymal stromal cells. J Bone Jt Surg Br 2006;88:1236–44.
[44] van Osch GJ, Brittberg M, Dennis JE, Bastiaansen-Jenniskens YM, Erben RG, Konttinen YT, et al. Cartilage repair: past and future–lessons for regenerative medicine. J Cell Mol Med 2009;13:792–810.
[45] Nauta AJ, Fibbe WE. Immunomodulatory properties of mesenchymal stromal cells. Blood 2007;110:3499–506.
[46] Rasmusson I. Immune modulation by mesenchymal stem cells. Exp Cell Res 2006;312:2169–79.
[47] Nasef A, Ashammakhi N, Fouillard L. Immunomodulatory effect of mesenchymal stromal cells: possible mechanisms. Regen Med 2008;3:531–46.

Acta Biomaterialia 8 (2012) 2340–2347

Contents lists available at SciVerse ScienceDirect

Acta Biomaterialia

journal homepage: www.elsevier.com/locate/actabiomat

Development and evaluation of tetrapod-shaped granular artificial bones

Sungjin Choi [a,b,*,1], I-li Liu [b,1], Kenichi Yamamoto [a], Kazuyo Igawa [c], Manabu Mochizuki [b], Takamasa Sakai [c], Ryosuke Echigo [b], Muneki Honnami [b], Shigeki Suzuki [d], Ung-il Chung [a,c], Nobuo Sasaki [b]

[a] Center for Disease Biology and Integrative Medicine, Graduate School of Medicine, The University of Tokyo, 7-3-1 Hongo, Bunkyo-ku, Tokyo 113-0033, Japan
[b] Laboratory of Veterinary Surgery, Graduate School of Agricultural and Life Sciences, The University of Tokyo, 1-1-1 Yayoi, Bunkyo-ku, Tokyo 113-8657, Japan
[c] Department of Bioengineering, School of Engineering, The University of Tokyo, 7-3-1 Hongo, Bunkyo-ku, Tokyo 113-0033, Japan
[d] NEXT21 K.K., 3-38-1 Hongo, Bunkyo-ku, Tokyo 113-0033, Japan

ARTICLE INFO

Article history:
Received 30 September 2011
Received in revised form 20 February 2012
Accepted 23 February 2012
Available online 2 March 2012

Keywords:
Bone graft
Calcium phosphate
Intergranular pores
Mechanical properties
Tetrapod

ABSTRACT

We have developed a novel form of granular artificial bone "Tetrabones" with a homogeneous tetrapod shape and uniform size. Tetrabones are four armed structures that accumulate to form the intergranular pores that allow invasion of cells and blood vessels. In this study we evaluated the physicochemical characteristics of Tetrabones in vitro, and compared their biological and biomechanical properties in vivo to those of conventional β-tricalcium phosphate (β-TCP) granule artificial bone. Both the rupture strength and elastic modulus of Tetrabone particles were higher than those of β-TCP granules in vitro. The connectivity of intergranular pores 100, 300, and 400 μm in size were higher in Tetrabones than in the β-TCP granules. Tetrabones showed similar osteoconductivity and biomechanical stiffness to β-TCP at 2 months after implantation in an in vivo study of canine bone defects. These results suggest that Tetrabones may be a good bone graft material in bone reconstruction.

1. Introduction

Trauma, disease, and developmental abnormalities resulting in skeletal defects often incur considerable morbidity. Although the use of autogenous bone, as blocks or in granular form, has long been considered the gold standard in terms of grafting material, this approach has several disadvantages, including donor site morbidity and the restricted quantity and shape of the tissue [1,2]. For these reasons calcium phosphate-based artificial bone materials such as hydroxyapatite and tricalcium phosphate (TCP) have been widely used in clinical practice [3–6]. These materials are used in various forms, including blocks, pastes, and granules, depending on the indication and type of bone defect.

The ideal granular artificial bone should be biocompatible and biodegradable, and exhibit controlled porosity, good pore interconnectivity, and biomechanical strength [7]. However, it has not yet been established which type of granular calcium phosphate-based artificial bone materials possess the best osteoconductive potential and biomechanical properties [8]. One problem with conventional granular calcium phosphate-based artificial bones is that they have irregular shapes and sizes, which may compromise their performance. To circumvent this problem we have designed and fabricated a novel granular artificial bone taking advantage of its tetrapod shape.

In the field of civil engineering tetrapods are used to protect harbors against the force of the ocean and the consequent erosion, capitalizing on their high mechanical strength, low center of gravity, and stability to external forces [9]. These advantages led us to hypothesize that tetrapods could be scaled down for application as artificial bone. We expected that their structural characteristics would provide better mechanical stability and control over intergranular pores.

In this study we fabricated novel tetrapod shaped granular artificial bone (hereafter referred to as "Tetrabones") by injection molding using microparticles of α-tricalcium phosphate (α-TCP). We first studied the physicochemical characteristics of Tetrabones in vitro, and then evaluated its biological and biomechanical properties in a canine model *in vivo* in comparison with β-TCP granules, which are widely used in clinical practice.

2. Materials and methods

2.1. Fabrication of Tetrabones

2.1.1. Materials

A mix of 60/40 wt.% α-TCP powder (Taihei Chemical Industrial Co., Tokyo, Japan) and binder (composed of 55% olefin resin, 30%

* Corresponding author at: Laboratory of Veterinary Surgery, Graduate School of Agricultural and Life Sciences, The University of Tokyo, 1-1-1 Yayoi, Bunkyo-ku, Tokyo 113-8657, Japan. Tel.: +81 3 5841 5405; fax: 81 3 5841 8996.
E-mail address: tjdwls1101@hotmail.com (S. Choi).
[1] These authors should be regarded as joint first authors.

1742-7061/$ - see front matter © 2012 Acta Materialia Inc. Published by Elsevier Ltd. All rights reserved.
doi:10.1016/j.actbio.2012.02.019

wax, and 15% plasticizing materials) were compounded in a tumbler mixer (Neo TecsK03P), and then mixed at room temperature in a rotating drum tumbler mixer for 5 h.

2.1.2. Fabrication of Tetrabones

Injection molds were prepared to fabricate 1 mm sized tetrapods, and the α-TCP powders were molded using an injection molding machine (J34AD, Japan Steel Works, Tokyo, Japan), Molded products were then degreased and calcined. The detailed parameters for the injection molding, degreasing, and calcination processes are given in Table 1.

The degreased and calcined products were soaked in 0.2 M succinic acid for 24 h to form octacalcium phosphate (OCP), rinsed twice with distilled water, dried under reduced pressure, and sterilized by electron beam irradiation at 25 kGy to give the final Tetrabone product.

β-TCP granules (Osferion®, size range 0.5–1.5 mm, porosity 75%; Olympus Biomaterial Corp., Tokyo, Japan) were used as the control material.

2.2. Material properties of Tetrabones

2.2.1. X-ray diffraction analysis

X-ray diffraction analysis (XRD) was performed using an X-ray diffractometer (Mini Flex 2, Rigaku, Japan) equipped with a CuK_α radiation source at 20 mA, scanning from $2\theta = 4$ to 60 °C. All samples were crushed before analysis. The results were compared with the International Center for Diffraction Data (ICDD) database.

2.2.2. Scanning electron microscopy

Scanning electron microscopy (SEM) was performed on pure α-TCP powders and the surface of injectionmolded products before and after succinic acid treatment, using a JCM-5700 scanning electron microscope (JEOL, Tokyo, Japan). Images were obtained at 1.2 keV accelerating voltage and 20 mA current.

2.2.3. Mechanical testing

The rupture strength of single Tetrabones and single β-TCP granules were measured with a rheometer (CR-500DX, Sun scientific Co., Japan). A single particle of each artificial bone was placed on the slab of the rheometer. The rod was loaded at 3 mm min^{-1} until the particle ruptured, and the rupture strength when each specimen broke was measured ($n = 4$).

For elastic modulus evaluation Tetrabones and β-TCP granules were embedded in cylindrical molds 5 mm in diameter and 10 mm long, and each mold was placed on the slab of an Instron universal testing machine (Instron-3365, Instron Corp., Norwood, MA). Arod 5 mm in diameter was loaded into the mold at 0.5 mm min^{-1}, and the elastic modulus measured ($n = 4$).

2.2.4. Analysis of size and connectivity of intergranular pores

Polymer beads used to simulate cells and blood vessels were provided by the Sekisui Plastics Corporation (Osaka, Japan). The beads were composed of cross-linked polymethyl methacrylate and had diameters of 100, 300, 400, and 600 μm.

The end of a 2.5 ml syringe barrel was cut to create a cylindrical tube and sealed with mesh. The plunger was pulled back and the rubber cap removed. The barrel was filled with 0.5 ml of Tetrabones or β-TCP granules, overlaid with 1.5 ml of the beads, and the plunger pushed back into the barrel. The end of the plunger was loaded with a 500 g weight and the syringe was vibrated using a vibrator for 2 min. The beads were collected as they exited the syringe and their weight measured ($n = 3$, Fig. 1). Additionally, mercury porosimetry was performed using a Micromeritics Autopore III 9510 mercury porosimeter (Micromeritics Instrument Corp., Norcross, GA) to compare the values of these methods.

Table 1
Detailed parameters of the Tetrabone fabrication process.

Injection molding	Degreasing	Calcination
Cylinder temperature 170–190 °C	Maximum temperature 500 °C	Maximum temperature 700 °C
Mold temperature 25–40 °C	Rate of temperature rise 87°Ch^{-1}	Rate of temperature rise 87°Ch^{-1}
Injection pressure 30–50 MPa	Holding time 1 h	Holding time 1 h
Injection velocity 0.3–0.5 s		
Screw revolution speed 1000 r.p.m.		

2.2.5. Cell viability

MC3T3-E1 cells were cultured on Tetrabones or β-TCP granules in standard medium (Dulbecco's modified Eagle's medium (DMEM) supplemented with 10 vol.% fetal bovine serum (FBS), 50 U ml^{-1} penicillin, and 50 mg ml^{-1} streptomycin) at 37 °C in a 5% CO_2 atmosphere. When the cells reached confluence the medium was changed to osteogenic medium (standard medium supplemented with 0.1 μM dexamethasone, 50 mM β-glycerophosphate and 50 μg ml^{-1} ascorbic acid). 7 days later the Tetrabones and β-TCP granules were stained with an alkaline phosphatasestaining kit (Takara Bio, Tokyo, Japan). The numbers of cells growing on the surface of the Tetrabones and β-TCP granules werecounted using a stereoscopic microscope.

2.3. In vivo experiments

2.3.1. Canine bone defect model

Seven healthy beagle dogs (10–12 kg body weight, 1–2 years of age) were purchased from Nosan Corporation (Kanagawa, Japan). General anesthesia was maintained with isoflurane, and fentanyl hydrate was continuously administered during and after surgery. The femoral medial condyle was exposed, and a tunnel defect 10 mm in diameter extending to the lateral cortex was created in the bilateral femur using a power surgery drill (IMEX™ Veterinary Inc., Longview, TX). After irrigation of the defect with sterile saline, Tetrabonesor β-TCP granules were implanted into the defect ($n = 5$ each), or, in the control group, nothing was implanted ($n = 4$). After implantation the joint capsule, fascia lata, subcutaneous tissue, and skin were sutured. An antibiotic (cefazolin, 20 mg kg^{-1} subcutaneously twice daily) and an analgesic (buprenorpine, 15 μg kg^{-1} intramuscularly twice daily) were administered for 3 days after implantation. This study was conducted under the Guidelines of the Animal Care Committee of the Graduate School of Agricultural and Life Sciences, the University of Tokyo.

2.3.2. Biomechanical analysis

8 weeks after implantation the distal part of the femur was excised, and the surrounding tissue removed. The normal femur was used as the positive control ($n = 5$). The specimes was fixed with bone cement with the longitudinal axis of the bone defect vertical to the slab of a rheometer (CR-500DX, Sun Scientific Co., Japan), and a rod 5 mm in diameter was preloaded on the surface of the defect site at 1 N force. The specimen was loaded at 3 mm min^{-1}, and stopped when displacement reached a depth of 0.25 mm to avoid destruction of the specimen. Force–displacement changes in the bone defect were observed and the stiffness calculated from the slope of the linear region of the resulting force–displacement curve.

2.3.3. Histological analysis

After the biomechanical analysis the bone around the implant sites was trimmed and fixed with 10% neutralized formaldehyde

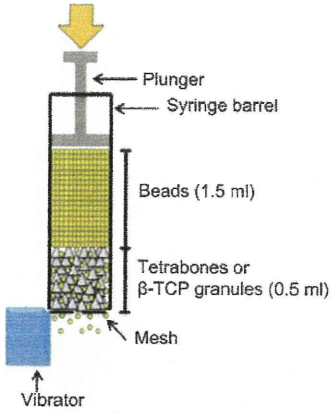

Fig. 1. A novel method of evaluating the size and connectivity of intergranular pores.

for 1 week, then demineralized with Plank-Rychlo decalcifying solution for 20 weeks. It was then embedded in paraffin, cut into 7 μm thick longitudinal sections, and stained with Masson's Trichrome.

To evaluate the new bone tissue a picture of the entire specimen was taken under a light microscope (Biozero, Keyence, Japan). The ratios of new bone area and distribution were measured using ImageJ software (National Institutes of Health, Bethesda, MD). To evaluate the new bone area we measured only the new bone tissue showing a calcified dense matrix which stained deep blue at high magnification. To evaluate the distribution the extended margins of the new bone tissue were measured, and the outer area of the margins were defined as the distribution of new bone tissue.

2.4. Statistical analysis

All data are expressed as means and standard deviations. Statistical analysis was performed using SPSS software (IBM, New York, NY). One-way analysis of variance was performed to compare the properties of Tetrabones and β-TCP granules, with Tukey's post hoc test applied for the biomechanical analysis in vivo. P values of less than 0.05 were considered statistically significant.

3. Results

3.1. Fabrication of Tetrabones

Tetrabones of homogeneous shape and size (1 mm) were fabricated by injection molding and succinic acid treatment. The macromorphology of Tetrabones was visualized by SEM, which confirmed their uniform size and shape (Fig. 2A). In contrast, β-TCP granules showed heterogeneous shapes and sizes (Fig. 2B).

3.2. Material properties of Tetrabones

3.2.1. X-ray diffraction analysis

XRD was performed to confirm OCP formation on Tetrabones by succinic acid treatment. The XRD patterns of pure α-TCP powder and the injectionmolded products before and after succinic acid treatment are shown in Fig. 3. The XRD patterns of the injectionmolded products before succinic acid treatment fitted the standard peak of α-TCP well. After succinic acid treatment the main peak observed at $2\theta = 4.70°$ was assigned to OCP, while peaks at around $2\theta = 30°$ indicated mainly TCP and other calcium phosphate complexes. These results indicate that some part of Tetrabones was recrystallized into OCP and other calcium phosphates by succinic acid treatment. The XRD of β-TCP granules showed pure β-TCP peaks.

3.2.2. Assessment of surface structure

SEM was also performed to observe the surface structure of Tetrabones. SEM of the injectionmolded products before succinic acid treatment revealed globular particles similar to pure α-TCP powder (Fig. 4A and B). After succinic acid treatment thin plate-like crystals characteristic of OCP were observed on the surface of the Tetrabones (Fig. 4C and Supplementary Fig. 1). These data suggest that α-TCP on the surface of Tetrabones was recrystallized into OCP, while the inner structure beneath the surface was mainly TCP and other calcium phosphate complexes, which may support the XRD data.

3.2.3. Mechanical testing

To assess the mechanical properties of Tetrabones and β-TCP granules the rupture strength of single granules and the elastic modulus of aggregates were evaluated using a rheometer and a universal testing machine, respectively.

The rupture strength of single Tetrabone particles was 3.45 ± 0.42 N and that of β-TCP granules was 1.20 ± 0.42 N (Fig. 5A). The elastic modulus of aggregated particles was 65.15 ± 7.98 MPa for the Tetrabones and 7.85 ± 3.43 MPa for the β-TCP granules (Fig. 5B). Both parameters were significantly higher in the Tetrabone group than in the β-TCP granule group ($P < 0.05$).

3.2.4. Analysis of size and connectivity of intergranular pores

The weights of 100 μm diameter beads passing through the Tetrabone packed or β-TCP granule packed syringes were 0.236 ± 0.030 and 0.135 ± 0.034 g, respectively ($P < 0.05$); for the 300 μm beads these weights were 0.214 ± 0.014 and 0.010 ± 0.002 g ($P < 0.05$); for the 400 μm beads they were 0.046 ± 0.011 and 0.021 ± 0.005 g ($P < 0.05$). However, the 600 μm diameter beads did not pass through either material (Fig. 6A).

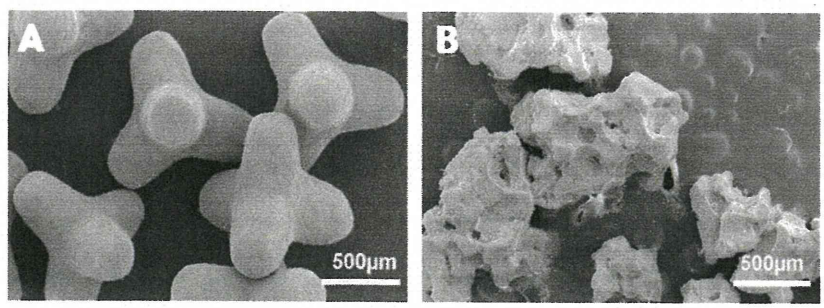

Fig. 2. Macromorphology (SEM image) of (A) Tetrabones and (B) β-TCP granules. Scale bar 500 μm.

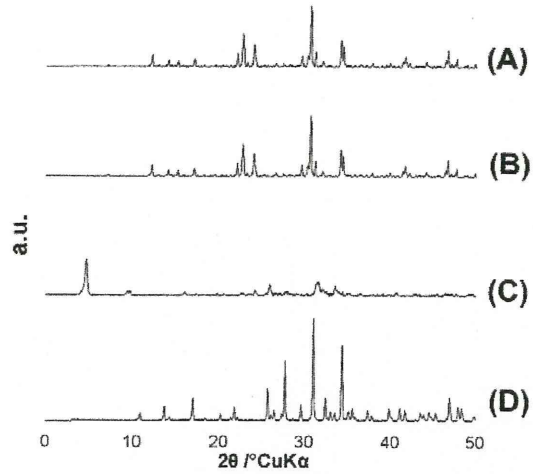

Fig. 3. XRD patterns of pure (A) α-TCP powder, injectionmolded products (B) before and (C) after succinic acid treatment (Tetrabones), and (D) β-TCP granules. The white arrowhead indicates a peak of α-TCP; the black arrowhead indicates a peak of OCP.

Thus the connectivity of the 100–400 μm intergranular pores was significantly higher in the Tetrabone group than in the β-TCP granule group, suggesting that Tetrabones have intergranular pores that may be more supportive of cell and vascular invasion than conventional artificial bone materials.

Using mercury porosimetry there were no significant differences between these values for the 100–300, 300–400 and 400–500 μm beads (Fig. 6B).

3.2.5. Cell viability

To evaluate the effect of Tetrabones on cell viability the number of cells attached to the surface of the artificial bone was counted after 7 days in culture. The number of attached cells was $17.40 \pm 1.67\ mm^{-2}$ in the Tetrabone group and $16.00 \pm 1.41\ mm^{-2}$ in the β-TCP granule group (Fig. 7), which was not significantly different. These data suggest that Tetrabones and β-TCP granules show comparable abilities to support viable attached cells.

3.3. In vivo experiments

3.3.1. Biomechanical analysis

The biomechanical properties of Tetrabones were evaluated 8 weeks after implantation in vivo, by measuring the stiffness of a canine femoral defect filled with Tetrabones or β-TCP granules. The resulting force–displacement curves for each specimen are shown in Fig. 8A. The stiffness was $27.99 \pm 5.87\ N\ mm^{-1}$ for the normal bone group, $21.59 \pm 2.43\ N\ mm^{-1}$ for the Tetrabone implantation group, $2.91 \pm 2.15\ N\ mm^{-1}$ for the β-TCP granule implantation group, and $1.41 \pm 1.91\ N\ mm^{-1}$ for the control group (Fig. 8B), respectively. The stiffness of the normal bone group was significantly higher than the other groups, and the Tetrabone implantation group was significantly higher (7.4-fold, $P < 0.05$) than those of the β-TCP granule implantation and control groups. There was no significant difference between the β-TCP granule implantation group and the control group.

3.3.2. Histological analysis

The implantation sites of the Tetrabone implanted and β-TCP granule implanted femurs were analyzed histologically for evidence of new bone growth. The surface of the Tetrabones was found to be surrounded by new bone tissue, which was present in most of the defect area (Fig. 9A). Moreover, most of the intergranular pores were filled with new bone tissue and bone marrow cells (Fig. 9D). In the β-TCP granule implantation group there was abundant new bone tissue at the margins of the defect (Fig. 9B), while most of the tissue in the central area was fibrous tissue (Fig. 9E). In the control group a large dead space without any tissue was observed in the central area (Fig. 9C), and at the marginal site most of the tissue was fibrous tissue (Fig. 9F).

The ratios of new bone area in the bone defects were $16.23 \pm 2.31\%$ in the Tetrabone implantation group, $15.78 \pm 3.11\%$ in the β-TCP granule implantation group and $6.97 \pm 2.64\%$ in the control group, respectively. Those of the Tetrabone implantation

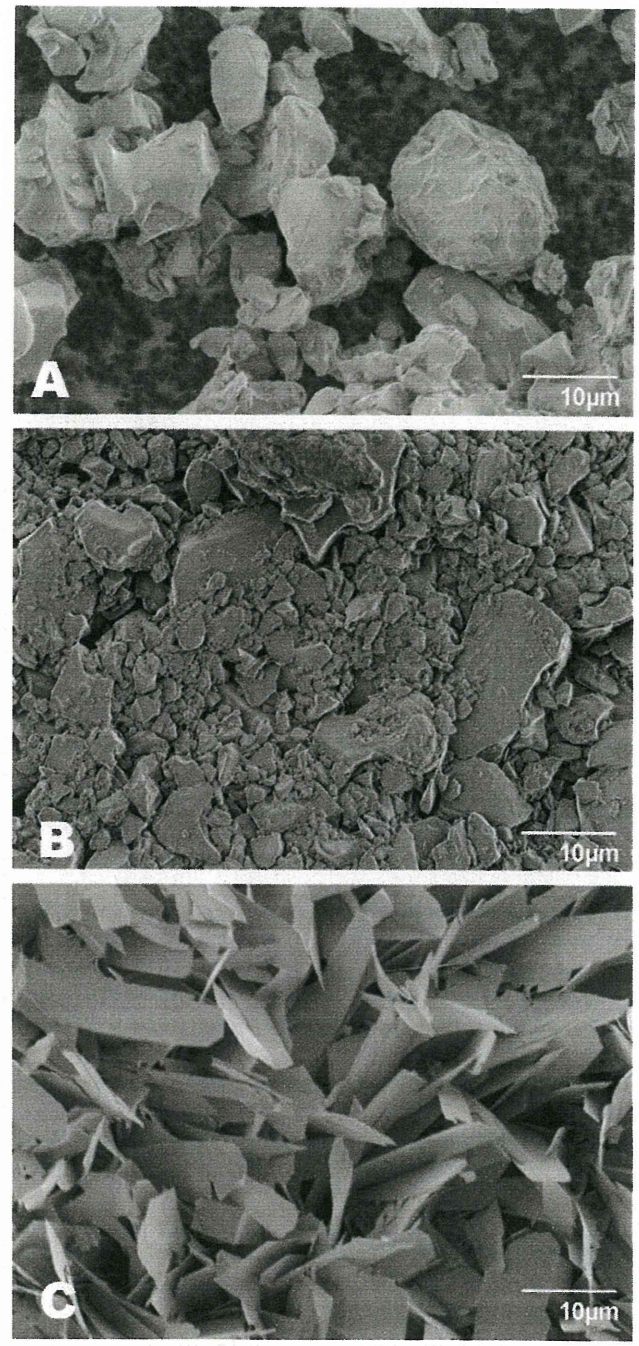

Fig. 4. SEM images of (A) pure raw α-TCP powder, injectionmolded products (B) before succinic acid treatment and (C) after succinic acid treatment (Tetrabones). Scale bar 10 μm.

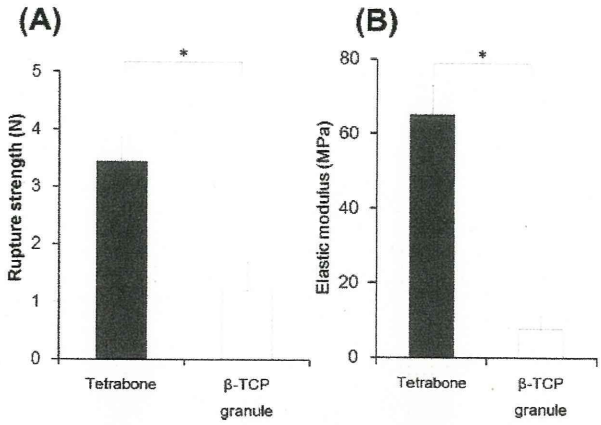

Fig. 5. Mechanical properties of Tetrabones and β-TCP granules. (A) Rupture strength of a single particle of Tetrabone and β-TCP granules and (B) the elastic modulus of assembled particles of Tetrabones and β-TCP granules. *$P < 0.05$.

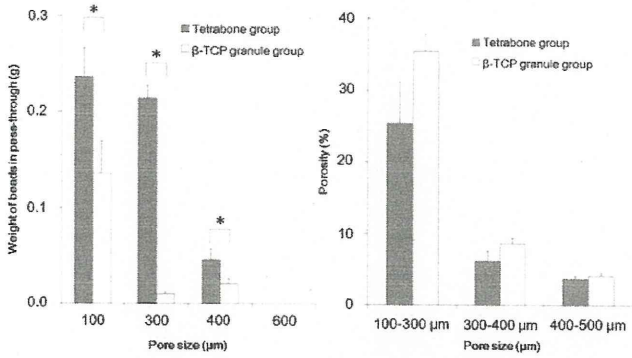

Fig. 6. Analysis of the size and connectivity of intergranular pores using (A) microbeads and (B) mercury porosimetry in the Tetrabone group and the β-TCP granule group. *$P < 0.05$.

and the β-TCP granule implantation groups were significantly higher than that of the control group ($P < 0.05$), and there was no significant difference between those of the Tetrabones and β-TCP granule implantation groups. The ratios of new bone distribution in the bone defects were 89.68 ± 7.34% in the Tetrabone implantation group, 60.87 ± 12.39% in the β-TCP granule implantation group and 44.98 ± 12.09% in the control group, respectively. Those of the Tetrabone implantation group and the β-TCP granule implantation group were significantly higher than that of the control group ($P < 0.05$), and that of the Tetrabone implantation group was significantly higher than that of the β-TCP granule implantation group ($P < 0.05$, Fig. 9G).

The Tetrabone implantation group showed a new bone area comparable with that of the β-TCP granule implantation group, and new bone tissue was homogeneously distributed in bone defects in the Tetrabone implantation group, while it was heterogeneously distributed in the β-TCP granule implantation group.

4. Discussion

Calcium phosphate granules of various shapes and sizes have been used widely in clinical practice [10–12]. However, they can only be used for non-load-bearing sites due to their poor biomechanical strength [8,13]. The four-armed tetrapod structure was designed by civil engineers to dissipate force and reduce displacement by allowing a random distribution of tetrapods to mutually

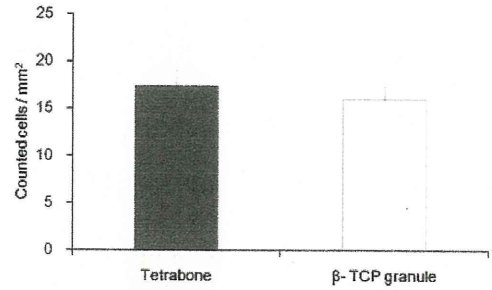

Fig. 7. Cell viability on Tetrabones and β-TCP granules. Seven days after osteogenic culture the number of MC3T3-E1 cells per square millimeter of Tetrabones or β-TCP granules was determined by ALP staining.

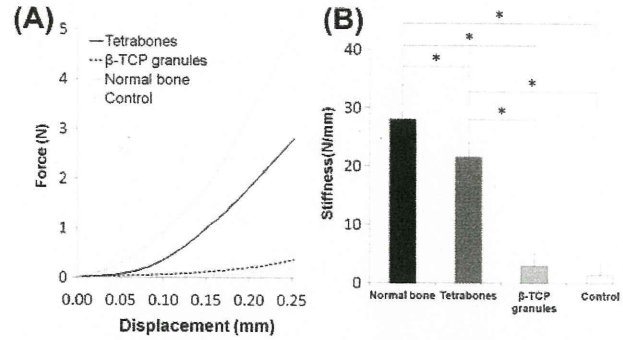

Fig. 8. Biomechanical properties of normal bone, non-treated defects and the implantation sites of Tetrabones and β-TCP granules 2 months after implantation. (A) Force–displacement curve and (B) stiffness of the bone defects. *$P < 0.05$.

interlock. We hypothesized that the same principle could be applied to artificial bone graft materials and thus developed tetrapod-shaped Tetrabones. In the present study we have evaluated their mechanical strength, their ability to retain their shape in bone defects in vivo, and the formation of intergranular pores that allow invasion by cells and blood vessels. Tetrabones showed greater mechanical strength than β-TCP granules as both single units and in aggregates, which can be attributed to both its composition and shape. First, the α-TCP crystals on the Tetrabone surface recrystallize as OCP after succinic acid treatment, which has high mechanical strength [14]. Second, as described above, the load force on accumulated Tetrabones was likely evenly dissipated due to the mechanical stability imparted by their homogeneous and symmetrical structure.

In addition to its high mechanical strength, OCP is known to have excellent biocompatibility, osteoconductivity, and biodegradability [15–17]. Our in vitro experiments with MC3T3-E1 cells under osteogenic culture conditions revealed that cells attached to OCP-coated Tetrabones had comparable viability to those attached to β-TCP granules. In a previous study OCP was shown to facilitate the differentiation of osteogenic cells into osteoblastic cells, although the mechanism by which this occurs remains unknown [18]. These characteristics likely contributed to the good osteoconductivity displayed by Tetrabones.

The size and connectivity of intergranular pores are important factors for bone regeneration because they facilitate vascular and tissue in growth [19,20]. In addition, Tamai et al. have reported that pore interconnectivity is a primary determinant of osteoconductivity [21]. We hypothesized that their homogeneous shape and size would allow accumulated Tetrabones to create more effective intergranular pores than β-TCP granules for cell and vascular invasion. We tested this hypothesis by devising a novel

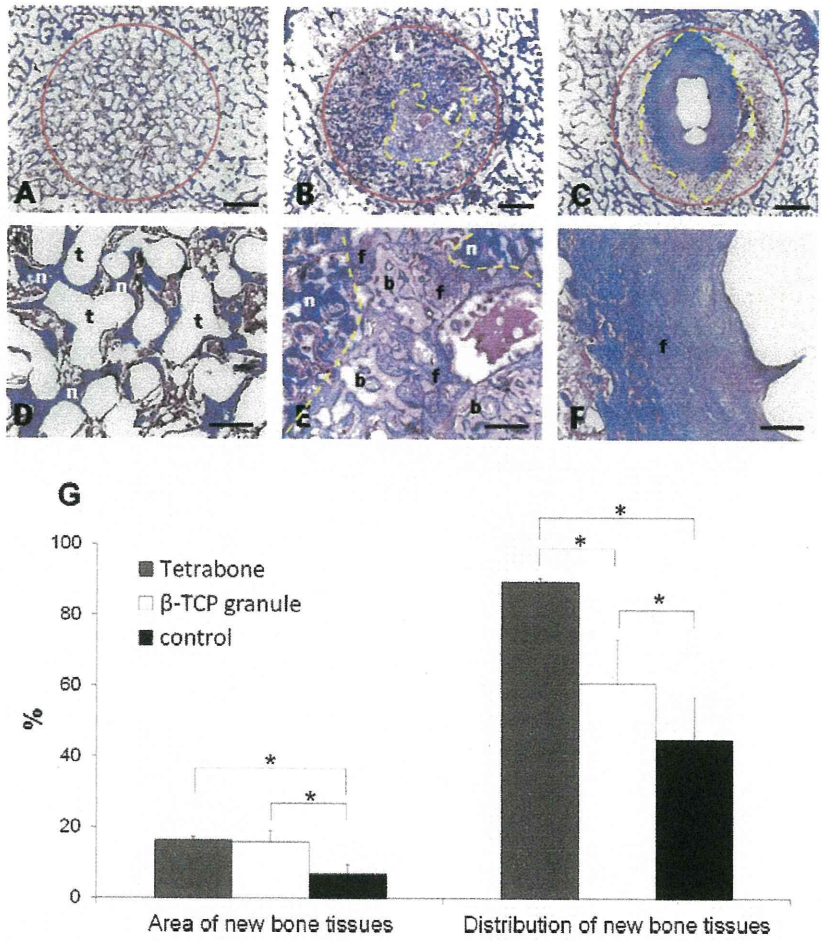

Fig. 9. Histological findings for the implantation sites of each group. Masson Trichromestaining 2 months after implantation of (A and D)Tetrabones and (B and E) β-TCP granules and (C and F) non-treated bone. *$P < 0.05$. Solid line, the bone defect; dotted line, the extended margin of new bone tissue; n, the new bone tissues; f, fibrous tissues; b, β-TCP granule; t, Tetrabone. Scale bar2 mm (A–C); 500 μm (D–F).

method using microbeads to assess the intergranular pores sizes in Tetrabones and β-TCP granules. Mercury porosimetry is a typical method to evaluate pore sizes from 0.1 to 1000 μm and has been widely used to evaluate the porous structure of various calcium phosphate materials [21,22]. However, this method is not suitable for porosity evaluation when the pore connection has a inlet that narrows or a pathway with an hourglass or ink bottle form [23,24]. If an inlet or a pathway is smaller than the diameter of a cell, although there is sufficient space beyond the inlet, the space may be accessible to mercury but inaccessible to cells and blood vessels, thus creating a "dead space" within the tissue. Mercury porosimetry may overestimate the intergranular pores by including these dead spaces. To address this problem we used a novel method to evaluate the size and connectivity of the intergranular pores using microbeads passing through Tetrabones or β-TCP granules to simulate passage of cells and blood vessels through the pores. We could evaluate the connectivity of the intergranular pores excluding those pores smaller than a certain size by this novel method. In this study, although the mercury porosimetry results indicated no significant differences between two groups, the results of the novel method using microbeads indicated higher intergranular pore connectivity in the Tetrabone group. These results using the novel method agreed with the histological findings, which showed homogeneously distributed new bone tissue in the Tetrabone implantation group and heterogeneously distributed new bone tissue in the β-TCP granule implantation group. These data suggest that this novel method using microbeads may be more appropriate to evaluate the size and connectivity of intergranular pores than mercury porosimetry. This is a simple method using microbeads and a syringe and is effective in evaluating the connectivity of intergranular pores, although this cannot measure the total porosity of the materials.

β-TCP granules, having a heterogeneous size and shape, showed fewer effective intergranular pores than did Tetrabones. It is possible that smaller β-TCP granules were situated between larger granules, thus obstructing the connection of intergranular pores. It is also known that granules with a homogeneous shape are less pro-inflammatory and facilitate faster bone in growth than granules having a heterogeneous shape [25].

Several studies have examined the pore size of calcium phosphate implants, and have reported that a pore size of about 100–1000 μm is adequate for bone regeneration [26–29], with a minimum pore size of 50 μm being recommended [30]. In the present study the accumulated Tetrabones were porous to 100, 300, and 400 but not 600 μm beads, suggesting that the intergranular pore size is less than 600 μm. Kuhne et al. reported that larger pore sizes led to higher osteoconductivity [26]. However, larger pore sizes also reduce the mechanical strength of the implant [31], suggesting that, on balance, a larger pore size is not necessarily a desirable property. There is a granular material called JAX™ (Smith and Nephew Orthopaedics Ltd.) similar to Tetrabone. JAX™ is 4 mm in diameter and made of β-TCP, and has a six-armed structure to provide 55% intergranular porosity ranging from 40 to 3000 μm. It has been reported that JAX™ has good osteoconductivity, and

has also been used as a drug delivery system in combination with osteogenic cells and anosteoinductive factor in previous studies [32,33]. However, it is limited to use for non-load-bearing defects because of its fragility [34]. In this study Tetrabone showed high mechanical strength in vitro and in vivo, suggesting potential application for load-bearing defects. Further study is needed to compare Tetrabones and JAX™ by investigating the mechanical properties, granule sizes (1 and 4 mm), number of arms (four or six), intergranular pore sizes and connections (under 600 and under 3000 μm).

β-TCP granules have been shown to have excellent osteoconductivity due to their superior biocompatibility and biodegradability in vivo [35,36]. In this study the β-TCP granule implantation group showed abundant new bone tissue in bone defects, as in previous studies. However, the new bone tissue was heterogeneously distributed. These phenomena may result from this particular bone defect model and a short observation period. In this study the observation period may not have been long enough to fully regenerate new bone tissue in the β-TCP granules implantation group. However, over a longer period some β-TCP granules might biodegrade in vivo before bone formation, and they may also lose their osteoconductive function and mechanical strength [37]. Actually, in the β-TCP granule implantation group there was less new bone tissue in the central area of the defect, with more fibrous tissue. The Tetrabone implantation group showed homogeneously distributed new bone tissue with less fibrous tissue, although the new bone area was comparable in both groups. This may indicate that Tetrabones have more connected intergranular pores. The larger connected intergranular pores of Tetrabones provide an effective scaffold, and facilitate more new bone tissue in the central area of the defects.

Several groups have performed biomechanical analyzes of the implantation site of artificial bones using bending or compression tests [38,39]. These methods are destructive and thus do not allow further evaluation of the sample. In this study we used a non-destructive method to assess biomechanical strength, which allowed subsequent histological analysis to be performed on the same samples. A similar method has been used to evaluate spine stiffness [40,41]. In an earlier preliminary study using cadaver samples we confirmed that elastic deformation was exhibited at 0.25 mm displacement without structural destruction. Therefore, we measured the stiffness up to 0.25 mm displacement. Although this method measures only stiffness, it still provides useful information to help explain the mechanical properties of the implant site.

In this study we used conventional β-TCP granules, having a heterogeneous size and shape, as the control. However, these two materials are not only different in size and shape, but also in surface structure and biodegradability due to their chemical compositions and different packing densities and surface areas when they form aggregates. Since these factors may influence the bone healing process in vivo further study should be performed taking these factors into consideration.

5. Conclusions

We succeeded in fabricating uniform 1 mm sized tetrapod shaped granular artificial bone coated with OCP, which we named Tetrabones. Tetrabones has a higher mechanical strength than conventional β-TCP granules in vitro, and, when forming aggregates, formed intergranular pores of an appropriate size and connectivity for cell and vascular invasion. Tetrabone implantation provided proper biomechanical properties to stabilize a bone defect and induce homogeneously distributed new bone tissue in vivo due to their proper intergranular pore connection after 2 months implantation. We conclude that Tetrabones have appropriate biomechanical properties and osteoconductive potential and may be a good bone graft material for bone reconstruction comparable with conventional granular artificial bone.

Acknowledgements

This research was supported by the Japan Society for the Promotion of Science through the "Funding Program for WorldLeading Innovative R&D in Science and Technology (FIRST Program)", initiated by the Council for Science and Technology Policy.

Appendix A. Supplementary data

Supplementary data associated with this article can be found, in the online version, at doi:10.1016/j.actbio.2012.02.019.

References

[1] Arrington ED, Smith WJ, Chambers HG, Bucknell AL, Davino NA. Complications of iliac crest bone graft harvesting. Clin Orthop Relat Res 1996;329:300–9.
[2] Sen MK, Miclau T. Autologous iliac crest bone graft: should it still be the gold standard for treating nonunions? Injury 2007;38(Suppl. 1):S75–80.
[3] Dorozhkin SV. Bioceramics of calcium orthophosphates. Biomaterials 2010;31(7):1465–85.
[4] Trombelli L, Heitz-Mayfield LJ, Needleman I, Moles D, Scabbia A. A systematic review of graft materials and biological agents for periodontal intraosseous defects. J Clin Periodontol 2002;29(Suppl. 3):117–35. discussion 160–112.
[5] Simpson D, Keating JF. Outcome of tibial plateau fractures managed with calcium phosphate cement. Injury 2004;35(9):913–8.
[6] Nair MB, Varma HK, Menon KV, Shenoy SJ, John A. Reconstruction of goat femur segmental defects using triphasic ceramic-coated hydroxyapatite in combination with autologous cells and platelet-rich plasma. Acta Biomater 2009;5(5):1742–55.
[7] Sopyan I, Mel M, Ramesh S, HKhalid KA. Porous hydroxyapatite for artificial bone applications. Sci Tech Adv Mater 2007;8:116–23.
[8] Costantino PD, Friedman CD, Jones K, Chow LC, Sisson GA. Experimental hydroxyapatite cement cranioplasty. Plast Reconstr Surg 1992;90(2):174–85. discussion 186–191.
[9] Franco L, Noli A, Paolo DG, Ercolani M. Concrete strength and durability of prototype tetrapods and dolosse: results of field and laboratory tests. Coast Eng 2000;40(3):207–19.
[10] Komuro Y. Use of calcium phosphate cement in craniofacial surgery. Med Postgraduates 2003;41(2):36–40.
[11] Garrido CA, Lobo SE, Turibio FM, Legeros RZ. Biphasic calcium phosphate bioceramics for orthopaedic reconstructions: clinical outcomes. Int J Biomaterials 2011;2011:129727.
[12] Chawla K, Lamba AK, Faraz F, Tandon S. Evaluation of beta-tricalcium phosphate in human infrabony periodontal osseous defects: a clinical study. Quintessence Int 2011;42(4):291–300.
[13] Linhart W, Briem D, Amling M, Rueger JM, Windolf J. Mechanical failure of porous hydroxyapatite ceramics 7.5 years after implantation in the proximal tibia. Unfallchirurg 2004;107(2):154–7.
[14] Komlev VS, Fadeeva IV, Barinov SM, Rau JV, Fosca M, Gurin AN, et al. Phase development during setting and hardening of a bone cement based on {alpha}-tricalcium- and octa calcium phosphates. J Biomater Appl. 2011. doi:10.1177/0885328210390403 [Epub ahead of print].
[15] Kamakura S, Sasano Y, Homma H, Suzuki O, Kagayama M, Motegi K. Implantation of octacalcium phosphate nucleates isolated bone formation in rat skull defects. Oral Dis 2001;7(4):259–65.
[16] Oonishi H, Hench LL, Wilson J, Sugihara F, Tsuji E, Kushitani S, et al. Comparative bone growth behavior in granules of bioceramic materials of various sizes. J Biomed Mater Res 1999;44(1):31–43.
[17] Chow LC. Next generation calcium phosphate-based biomaterials. Dent Mater J 2009;28(1):1–10.
[18] Suzuki O, Kamakura S, Katagiri T, Nakamura M, Zhao B, Honda Y, et al. Bone formation enhanced by implanted octacalcium phosphate involving conversion into Ca-deficient hydroxyapatite. Biomaterials 2006;27(13):2671–81.
[19] Eggli PS, Muller W, Schenk RK. Porous hydroxyapatite and tricalcium phosphate cylinders with two different pore size ranges implanted in the cancellous bone of rabbits. A comparative histomorphometric and histologic study of bony in growth and implant substitution. Clin Orthop Relat Res 1988;232:127–38.
[20] Ghanaati S, Barbeck M, Orth C, Willershausen I, Thimm BW, Hoffmann C, et al. Influence of beta-tricalcium phosphate granule size and morphology on tissue reaction in vivo. Acta Biomater 2010;6(12):4476–87.
[21] Tamai N, Myoui A, Tomita T, Nakase T, Tanaka J, Ochi T, et al. Novel hydroxyapatite ceramics with an interconnective porous structure exhibit superior osteo conduction in vivo. J Biomed Mater Res 2002;59(1):110–7.

[22] Kasten P, Beyen I, Niemeyer P, Luginbuhl R, Bohner M, Richter W. Porosity and pore size of beta-tricalcium phosphate scaffold can influence protein production and osteogenic differentiation of human mesenchymal stem cells: an in vitro and in vivo study. Acta Biomater 2008;4(6):1904–15.
[23] Yoshida R, Kishi T. Proposed approach of determination of pore continuity and suitable intrusion pressure based on step-by-step mercury intrusion porosimetery test. Seisankenkyu 2008;60(5):516–9.
[24] Diamond S. Mercury porosimetry an inappropriate method for the measurement of pore size distributions in cement-based materials. Cement Concrete Res 2000;30:1517–25.
[25] Paul W, Sharma CP. Development of porous spherical hydroxyapatite granules: application towards protein delivery. J Mater Sci Mater Med 1999;10(7): 383–8.
[26] Kuhne JH, Bartl R, Frisch B, Hammer C, Jansson V, Zimmer M. Bone formation in coralline hydroxyapatite. Effects of pore size studied in rabbits. Acta Orthop Scand 1994;65(3):246–52.
[27] Flautre B, Descamps M, Delecourt C, Blary MC, Hardouin P. Porous HA ceramic for bone replacement: role of the pores and interconnections – experimental study in the rabbit. J Mater Sci Mater Med 2001;12(8):679–82.
[28] Flatley TJ, Lynch KL, Benson M. Tissue response to implants of calcium phosphate ceramic in the rabbit spine. Clin Orthop Relat Res 1983;179 :246–52.
[29] Sanchez-Sálcedo S, Arcos D, Vallet-Regí M. Upgrading calcium phosphate scaffolds for tissue engineering applications. Key Eng Mater 2008;3777:19–42.
[30] Chang BS, Lee CK, Hong KS, Youn HJ, Ryu HS, Chung SS, et al. Osteoconduction at porous hydroxyapatite with various pore configurations. Biomaterials 2000;21(12):1291–8.
[31] Xu HH, Quinn JB, Takagi S, Chow LC, Eichmiller FC. Strong and macroporous calcium phosphate cement: effects of porosity and fiber reinforcement on mechanical properties. J Biomed Mater Res 2001;57(3):457–66.
[32] Clarke SA, Hoskins NL, Jordan GR, Henderson SA, Marsh DR. In vitro testing of Advanced JAX Bone Void Filler System: species differences in the response of bone marrow stromal cells to beta tri-calcium phosphate and carboxymethylcellulose gel. J Mater Sci Mater Med 2007;18(12): 2283–90.
[33] Clarke SA, Hoskins NL, Jordan GR, Marsh DR. Healing of an ulnar defect using a proprietary TCP bone graft substitute, JAX, in association with autologous osteogenic cells and growth factors. Bone 2007;40(4):939–47.
[34] Field JR, McGee M, Wildenauer C, Kurmis A, Margerrison E. The utilization of a synthetic bone void filler (JAX) in the repair of a femoral segmental defect. Vet Comp Orthop Traumatol 2009;22(2):87–95.
[35] Komaki H, Tanaka T, Chazono M, Kikuchi T. Repair of segmental bone defects in rabbit tibiae using a complex of beta-tricalcium phosphate, type I collagen, and fibroblast growth factor-2. Biomaterials 2006;27(29): 5118–26.
[36] Moore WR, Graves SE, Bain GI. Synthetic bone graft substitutes. Aust N Z J Surg 2001;71(6):354–61.
[37] Murakami Y, Honda Y, Anada T, Shimauchi H, Suzuki O. Comparative study on bone regeneration by synthetic octacalcium phosphate with various granule sizes. Acta Biomater 2010;6(4):1542–8.
[38] Zhang C, Wang J, Feng H, Lu B, Song Z, Zhang X. Replacement of segmental bone defects using porous bioceramic cylinders: a biomechanical and X-ray diffraction study. J Biomed Mater Res 2001;54(3):407–11.
[39] Chang RC, Kao AS. Biomechanical and histological studies of particulate hydroxylapatite implanted in femur bone defects of adult dogs. Int J Oral Maxillofac Surg 2000;29(1):54–61.
[40] Shirley D, Ellis E, Lee M. The response of posteroanterior lumbar stiffness to repeated loading. Man Ther 2002;7(1):19–25.
[41] Snodgrass SJ, Rivett DA, Robertson VJ. Measuring the posteroanterior stiffness of the cervical spine. Man Ther 2008;13(6):520–8.

DOI: 10.3727/096368912X640574

CT-0317 Accepted 09/10/2011 for publication in "*Cell Transplantation*"

Early-stage Foreign Body Reaction against Biodegradable Polymer Scaffolds Affects Tissue Regeneration during the Autologous Transplantation of Tissue Engineered Cartilage in the Canine Model

Yukiyo Asawa,[*] Tomoaki Sakamoto,[*] Makoto Komura,[†] Makoto Watanabe,[*] Satoru Nishizawa,[*] Yutaka Takazawa,[‡] Tsuyoshi Takato,[§] and Kazuto Hoshi[*]

[*] Departments of Cartilage & Bone Regeneration (Fujisoft), Tokyo University Graduate School of Medicine, Tokyo, Japan

[†] Department of Pediatric Surgery, Tokyo University Graduate School of Medicine, Tokyo, Japan

[‡] Department of Pathology, The University of Tokyo Hospital, Tokyo, Japan,

[§] Departments of Sensory & Motor System Medicine, Tokyo University Graduate School of Medicine, Tokyo, Japan

Running head: early reaction in cartilage regeneration

Address correspondence to: Kazuto Hoshi, M.D., Ph.D.

Department of Cartilage & Bone Regeneration (Fujisoft), Graduate School of Medicine,

The University of Tokyo, Hongo 7-3-1, Bunkyo-ku, Tokyo 113-8655, Japan.

Phone: +81-3-3815-5411 (ext. 37386), Fax: +81-3-5800-9891

E-mail: pochi-tky@umin.net